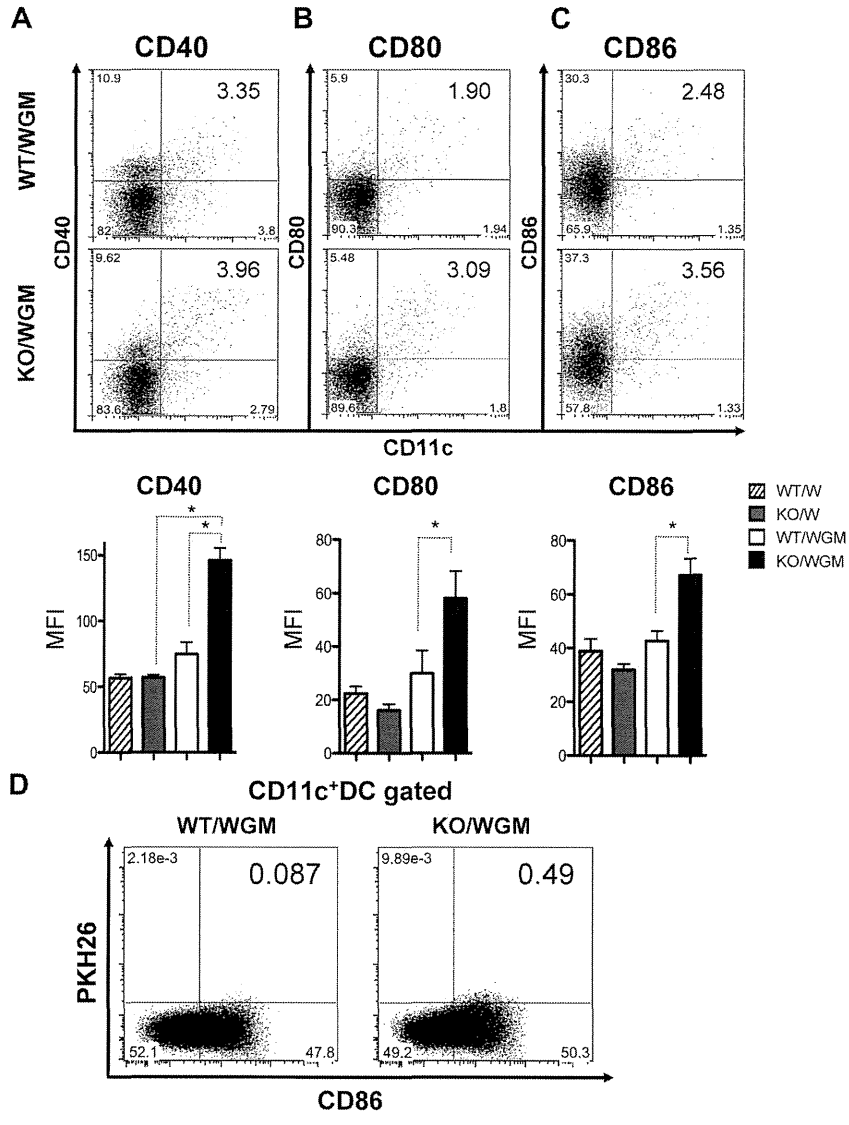

Figure 3. Absence of LTB4/BLT1 axis enhances maturation of DCs and recruitment of TAA-phagocytosed DCs into TDLNs in KO/WGM mice in early phase. Two left axillary TDLNs were harvested from WT/W, KO/W, WT/WGM, or KO/WGM mice on day 2 (CD80 and CD86) or day 4 (CD40) after the tumor challenge (n = 3-5 per group). Data are representative dot plots (top panel) and the averages of mean fluorescence intensity (bottom panel) for $CD11c^+$ cells expressing the following markers of (A) CD40, (B) CD80, or (C) CD86 in TDLNs harvested from 4 indicated experimental groups. Bar graphs represent mean ± SEM. *Significant difference ($P < .05$). (D) Migration of DCs that had phagocytosed TAAs to TDLNs in WT/WGM or KO/WGM mice on day 2 after the subcutaneous inoculation with PKH26-labeled WGM cells. Numbers in 2-dimensional dot plots reflect the positive ratio of $PKH26^+CD86^+$ cells relative to total $CD11c^+$ cells. Representative data from at least 3 independent experiments with similar results are shown.

Absence of LTB4/BLT1 axis in GM-CSF–induced antitumor immunity systemically enhances TAAs-specific Th1 and Th2 responses in intermediate phase

To characterize the immune-modulatory effects of the defective LTB4/BLT1 axis on GM-CSF–triggered adaptive immunity, the expression levels of inflammatory cytokines, IL-2, IFN-γ, TNF-α (Th1 cytokines), and IL-4 and IL-5 (Th2 cytokines) secreted from splenocytes harvested from KO/WGM mice were compared with those from WT/WGM mice. On the coculture with irradiated WEHI3B cells, the expression levels of IL-2, IFN-γ, TNF-α, IL-4, and IL-5 from KO/WGM mice, on day 10 after FTC, were increased compared with those from WT/WGM mice. Only levels of IL-4 were significantly altered. All other cytokines tested did not show significant differences between the 2 groups but exhibited the same tendency in 3 independent experiments (Figure 4A-E).

Absence of LTB4/BLT1 axis in GM-CSF-induced antitumor immunity increases diverse memory $CD4^+$ T subsets skewing Th balance toward Th2 and Th17 predominance with antitumor phenotype

We speculated that the defective LTB4/BLT1 axis could have a positive impact on phenotypic profile of different memory $CD4^+$ or $CD8^+$ T subset, which might account for the marked rejection of STC. Thus, we compared the rates of central memory T subset (T_{CM}) and effector memory T subset (T_{EM}) in TDLNs between WT/WGM and KO/WGM mice on day 46 in late phase. Surface marker of CD44 was used as memory phenotype. TDLNs harvested from KO/WGM mice contained significantly higher proportions of the $CD4^+CD44^+CD62L^+$ (T_{CM}) and $CD4^+CD44^+CD62L^-$ (T_{EM}) subsets relative to the total $CD4^+$ T-cell population compared with those from WT/WGM mice ($P < .05$; Figure 5A), suggesting that the defective LTB4/BLT1 axis could serve to generate long-surviving TAA-specific memory $CD4^+$ T cells. Subsequently, the proportion of Th1, Th2, and Th17 subsets in TDLNs and spleen in the late phase was evaluated between the 2 groups. The results showed that the frequency of Th2 and Th17 subset in TDLNs from KO/WGM mice increased by 32% and 47%, respectively, compared with that from WT/WGM mice (data not shown), indicating that the defective LTB4/BLT1 axis in GM-CSF–triggered immunity could cause a shift of the Th balance toward Th2 and Th17 predominance. Because IL-4 production fromTh2 cells is reported to be essential for maximal systemic antitumor immunity induced by GM-CSF–based tumor immunization,[4,28] we analyzed the total number of IL-4–producing $CD4^+$ T cells from TDLNs between the 2 groups. The total number of IL-4–producing

Th2 cells in TDLNs from KO/WGM mice was significantly higher than in WT/WGM mice ($P < .05$), suggesting that the defective LTB4/BLT1 axis facilitates effective induction of antitumor Th2 responses driven by GM-CSF (Figure 5B). To determine whether the Th17 subset has an in vivo antitumor activity, we treated recipient BALB/c mice with adoptive cell transfer of splenic Th17-skewed cells derived from WT/WGM or KO/WGM mice and subcutaneously challenged them with parental WEHI3B cells. Only the transfer of KO/WGM mice-derived Th17 cells significantly suppressed the WEHI3B tumor development compared with untreated and WT/WGM mice ($P < .05$; Figure 5C).

Furthermore, we evaluated the effect of the defective LTB4/BLT1 axis on regulatory T-cell subpopulations. The each percentage of $CD4^+CD25^+FoxP3^+$ regulatory T cells or $CD3^+CD4^+GITR^+$ cells between WT/WGM and KO/WGM mice was comparatively assessed, as GITR expression is constitutively up-regulated in regulatory T cells but not on resting $CD3^+CD4^+$ T lymphocytes.[29,30] The percentages of $CD4^+CD25^+Foxp3^+$ regulatory T cells in TDLNs and $CD3^+CD4^+GITR^+$ T cells in TDLNs and spleen from KO/WGM mice were more decreased than those from WT/WGM mice (Figure 5D-E).

Marked rejection of STC in KO/WGM mice is mainly attributed to $CD4^+$ T cells where memory Th subset possesses an antitumor phenotype

In vivo depletion of $CD4^+$ T, $CD8^+$ T, and NK cells was performed to determine which subsets are essential for the rejection of STC

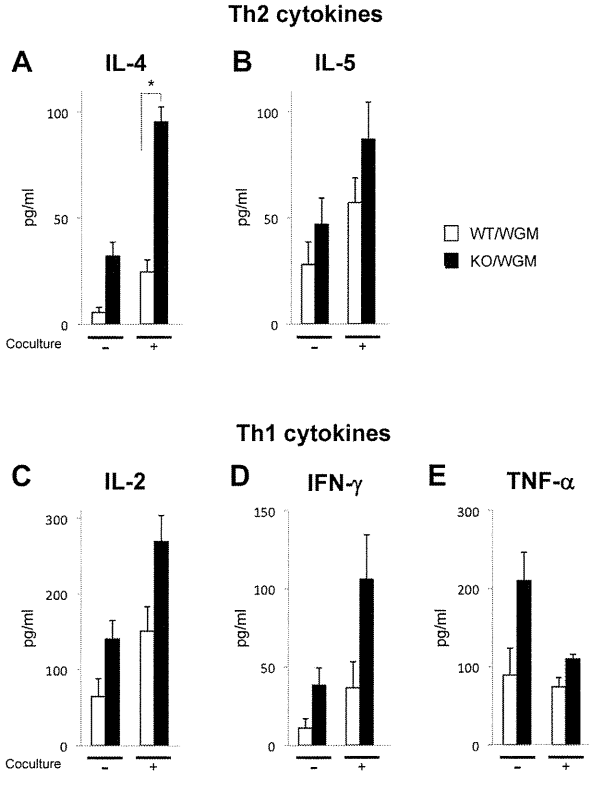

Figure 4. Absence of LTB4/BLT1 axis promotes systemic activation of TAA-specific Th1 and Th2 subsets in KO/WGM mice in intermediate phase. In vitro Th1/Th2 cytokine production profiles of splenocytes harvested from WT/W, KO/W, WT/WGM, or KO/WGM mice on day 10 after the FTC. Approximately 1×10^6 splenocytes harvested were cultured with or without 4×10^5 irradiated WEHI3B cells for 20 hours. The concentrations of mouse (A) IL-4, (B) IL-5, (C) IL-2, (D) IFN-γ, and (E) TNF-α in the culture supernatants (n = 3) were measured by cytometric bead array assay. Bar graphs represent mean ± SEM. *Significant differences ($P < .05$). Representative data from 3 independent experiments with similar results are shown.

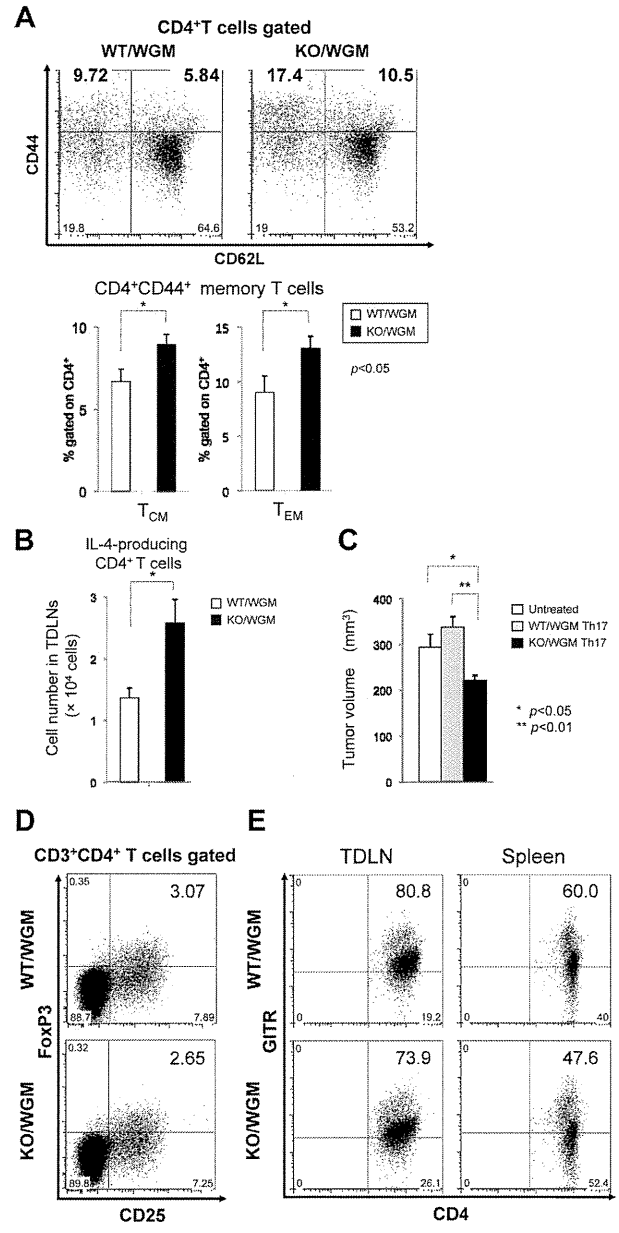

Figure 5. Absence of LTB4/BLT1 axis facilitates induction of diverse memory $CD4^+$ T subsets and polarized Th2/Th17 cells with antitumor phenotype in KO/WGM mice in late phase. TDLNs cells harvested from WT/WGM or WT/WGM mice (n = 3-5/group) on day 46 after the FTC were subjected to polychromatic flow cytometric analyses. (A) Dot plot profiles (top panels) and graphs (bottom panels) represent the percentages of $CD4^+CD44^+CD62L^+$ T_{CM} or $CD4^+CD44^+CD62L^-$ T_{EM} subset relative to the total $CD4^+$ T-cell population. Numbers in boldface in dot plot profiles show the representative percentages of T_{CM} and T_{EM} in WT/WGM and KO/WGM and are reflected to the graphs. (B) Bar graphs represent the total number of IL-4-producing T cells in TDLNs derived from WT/WGM and KO/WGM mice (n = 3 or 4). Combined data from 2 independent experiments are shown. (C) Th17 adoptive T-cell transfer (ACT) assay. Splenic $CD4^+$ T cells from WT/WGM or KO/WGM mice on day 46 were MACS-sorted and stimulated with plate-bound anti-CD3 mAb and soluble anti-CD28 mAb under Th17 condition. After 4 days of incubation, 1 million cells were intravenously transferred into recipient syngeneic BALB/c mice. On the next day, they received subcutaneous challenge with WEHI3B cells in the right flank. Bar graph represents the tumor volume (mm^3) of untreated, mice treated with WT/WGM mice- or KO/WGM mice-derived Th17 ACT, assessed on day 10 after the Th17 ACT therapy. (D-E) Phenotypic profile of immune-regulatory T cells in late phase. Shown are representative dot plots depicting the percentages of (D) $CD3^+CD4^+CD25^+FoxP3^+$ cells in TDLNs harvested from WT/WGM or KO/WGM mice, and of (E) $CD3^+CD4^+GITR^+$ T cells in TDLNs and spleen from WT/WGM or KO/WGM mice. Bar graphs represent the mean ± SEM. Significant differences: $^*P < .05$, $^{**}P < .01$. Representative data from 3 independent experiments with similar results or combined data (A-C) from 2 independent experiments are shown.

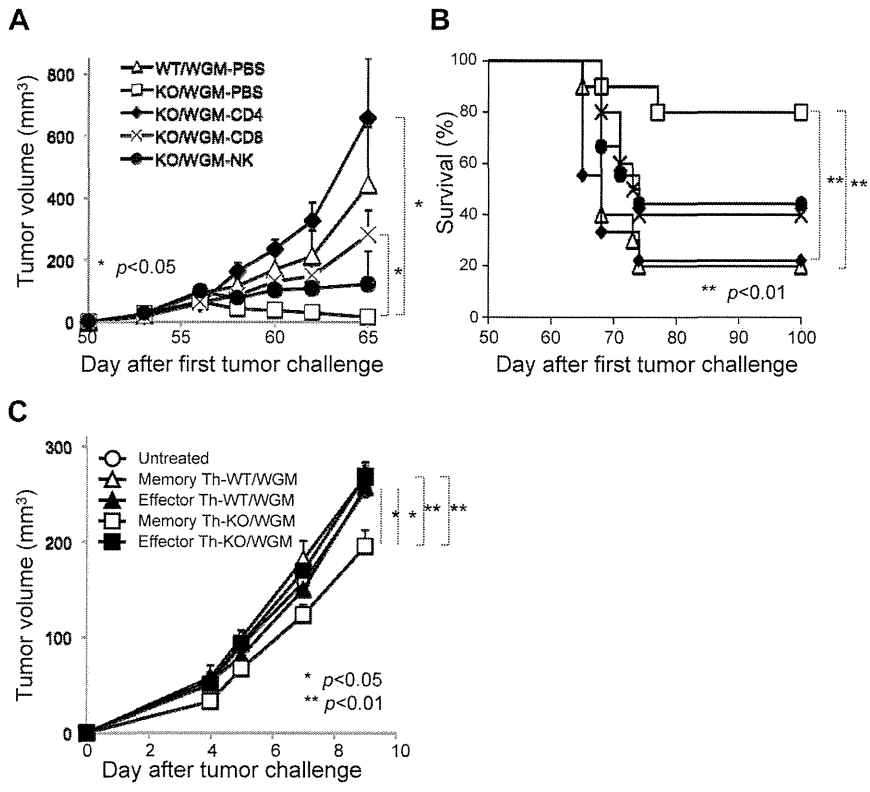

Figure 6. CD4$^+$ T cells mainly mediate the remarkable rejection of second tumor challenge with WEHI3B cells where memory CD44^{hi}CD4$^+$ T subset has an antitumor phenotype on adoptive cell transfer. All mice that had completely rejected the FTC with WGM cells were then subcutaneously inoculated with the STC on day 50 after the FTC, as described in Figure 1 (n = 4-6). For depletion of CD4$^+$ and CD8$^+$ T cells, mice received repeated intraperitoneal injections of anti–mouse-CD4 mAb or anti–mouse-CD8 mAb on days 3, 4, and 5 before the day of the STC and once every 3 days thereafter up to 13 times. For depletion of NK cells, mice received repeated intraperitoneal injections of rabbit anti-asialo GM1 antiserum 1 day before and 7 and 14 days after the STC. (A) Tumor volume was monitored and (B) a survival curve of the mice groups was examined. (C) For CD4$^+$ T-cell ACT therapy, 5×10^5 CD4$^+$CD44^{low} or CD4$^+$CD44^{hi} T cells harvested from spleen of WT/WGM or KO/WGM mice were flow cytometrically sorted on day 3 after the STC and intravenously injected into recipient syngeneic BLAB/c mice (n = 4-6). On the next day, they received subcutaneous challenge with 2×10^5 parental WEHI3B cells in the right flank. Bar graphs represent mean ± SEM. Significant differences: $^*P < .05$, $^{**}P < .01$. Representative or combined data from 2 independent experiments with similar results are shown.

seen in KO/WGM mice. Each depletion of CD4$^+$ T, CD8$^+$ T, or NK cells in KO/WGM mice significantly abrogated the antitumor effects compared with PBS-treated KO/WGM mice ($P < .05$). Importantly, KO/WGM mice depleted of CD4$^+$ T cells elicited rather accelerated tumor outgrowth (Figure 6A) and a significantly shorter survival (Figure 6B), with a significant decrease in number of mice that rejected the STC (Table 2), compared with WT/WGM mice, demonstrating that the long-lasting antitumor immunity seen in KO/WGM mice was largely dependent on CD4$^+$ T cells.

To determine whether the persistent antitumor memory observed in KO/WGM mice was memory CD4$^+$ T subset-dependent, we comparatively investigated therapeutic effects by adoptive T-cell transfer (ACT) between CD4$^+$CD44^{low} T cells (effector Th) and CD4$^+$CD44^{hi} T (memory Th) cells, both of which were sorted from spleens of WT/WGM or KO/WGM mice on day 3 after the STC. We treated mice with intravenous ACT therapy and, on the next day, challenged them with WEHI3B cells in the right flank. Either with or without ACT using KO/WGM mice-derived effector Th subset, WEHI3B tumors continued to grow, whereas ACT using KO/WGM mice-derived splenic memory Th subset significantly inhibited the WEHI3B tumor formation (Figure 6C). On the other hand, all ACT therapies using cells from WT/WGM mice manifested no antitumor activity. These results strongly indicated that memory Th subset has an important role in GM-CSF–induced antitumor memory immunity when the LTB4/BLT1 signaling is not present or dysfunctional.

Table 2. Effect of in vivo depletion of each immune subpopulation on the long-lasting rejection of the second tumor challenge

Group	Mice that rejected second tumor challenge, no. (%)*
WT/WGM-PBS	1/10 (10.0)†
KO/WGM-PBS	9/11 (81.8)
KO/WGM-CD4	1/10 (10.0)†
KO/WGM-CD8	3/11 (27.3)†
KO/WGM-NK	2/10 (20.0)†

Shown are combined pooled data from 2 independent experiments with similar results.

*Assessed at day 15 after the second tumor challenge with WEHI3B cells.

†χ^2 test ($P < .05$).

Discussion

Memory T cells respond promptly to delivered antigens and are critical in the induction of sustained antitumor immunity. They require less costimulation to be activated and release a broader spectrum of cytokines compared with naive T cells.[31] One of the major challenges for therapeutic improvement of cancer vaccines is to optimize persistent memory antitumor responses.

Numerous studies reported that leukotrienes are involved in carcinogenesis and tumor development.[24,25,32,33] However, the role of leukotriene-based signaling in tumor immunology, including memory immunity, has never been elucidated. In the current study, we are the first group to find that the defective LTB4/BLT1 signaling induces long-term antitumor memory responses after immunization with WGM cells, demonstrating that the LTB4/BLT1 axis is an adversary for maintaining GM-CSF–triggered antitumor memory responses as summarized in a schematic overview (Figure 7). Namely, blockade of the LTB4/BLT1 signaling elicited numerous positive effects on development of GM-CSF–triggered persistent antitumor memory immunity as follows:

1. The defective LTB4/BLT1 axis diminished the recruitment of immune-regulatory MDSCs into tumors in early phase (Figure 2B), probably because of abundant BLT1 expression in diverse myeloid cells, including MDSCs.[34]

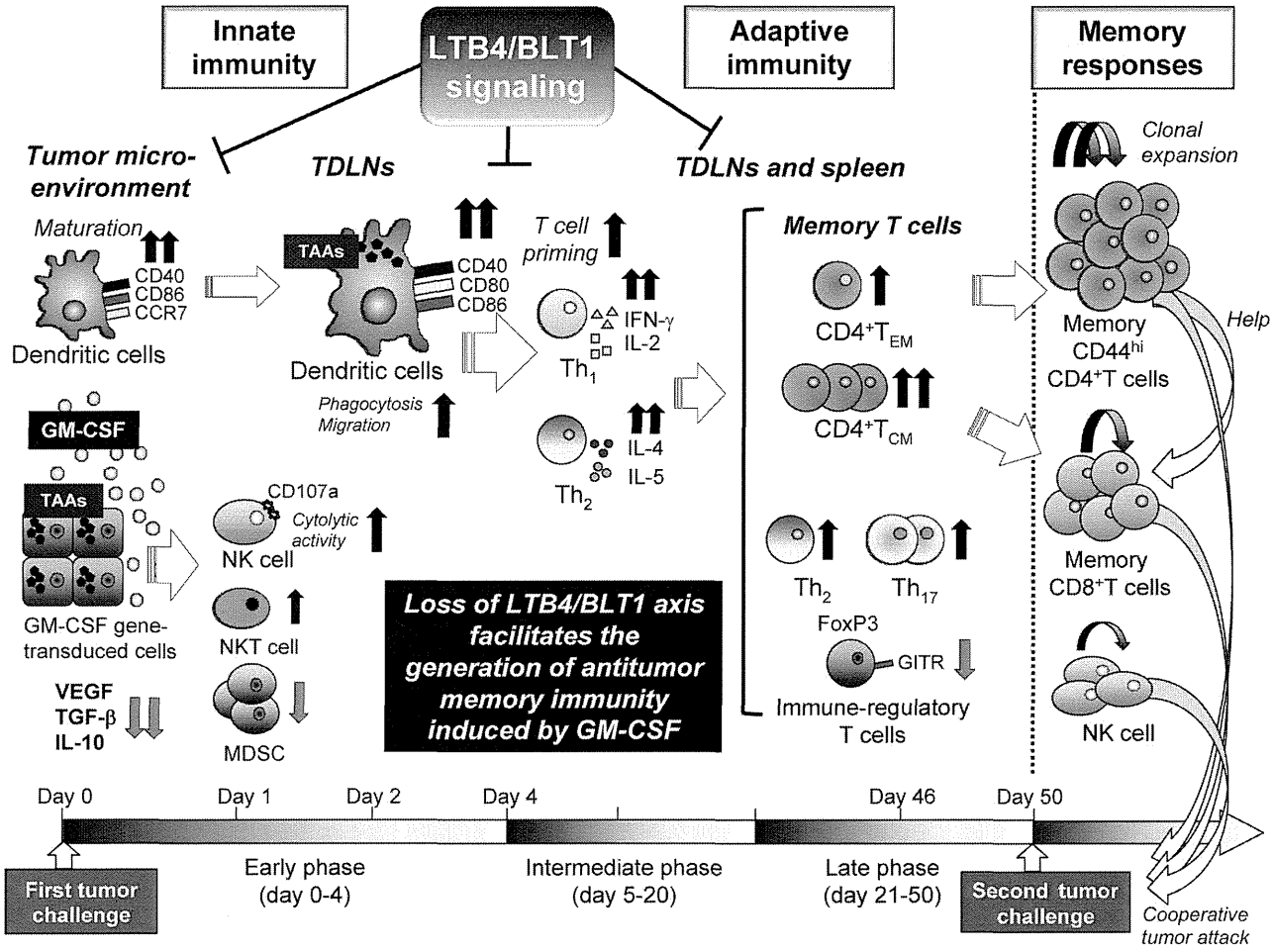

Figure 7. Schematic overview of the experimental results. This schematic overview illustrates the effects of the defective LTB4/BLT1 axis on the process of generation of antitumor memory immunity provoked by GM-CSF–transduced tumor cells in mice, and the molecular or cellular components that compose the immune system and are putatively relevant to this phenomenon.

2. The absence of LTB4/BLT1 axis increased recruitment of CD107a, a surrogate for lytic degranulation,[35] expressing cytolytic NK cells into tumors (Figure 2E), indicating its negative effects for tumoricidal ability activated by GM-CSF.
3. The defective LTB4/BLT1 signaling caused a synergistic effect on maturation, homing capacity of TAA-phagocytosed DCs into TDLNs (Figures 2F-H and 3A-D), and further enhanced the capacity of GM-CSF–sensitized DCs to stimulate $CD4^+$ T cells, but not $CD8^+$ T cells (Figure 2J-K), indicating its effective priming of helper T cell-predominant adaptive immunity. These positive effects on DCs were the result of the decreased expression of various immune-regulatory cytokines in tumor microenvironments (Figure 2I). On the contrary, others reported that LTB4 stimulation enhances DC migration and adaptive immune responses.[13] This discrepancy may stem from our use of GM-CSF gene-transduced tumor cells, although the detailed molecular crosstalk between LTB4/BLT1 and GM-CSF signaling remains unknown.
4. The absence of LTB4/BLT1 axis augmented the production of Th1 cytokine and Th2 cytokine from TAA-stimulated splenocytes harvested from GM-CSF–sensitized mice in intermediate phase (Figure 4). Conversely, Toda et al showed that functional BLT1 expression on DCs is important to initiate Th1-type immune response, indicating that GM-CSF–based immunization may bring about the conflicting outcome.[36]
5. The absence of LTB4/BLT1 axis increased the proportions of $CD4^+$ T_{CM} and $CD4^+$ T_{EM} subset in TDLNs in late phase before the STC (Figure 5A). As memory T cells possess the capacity to mount immediate recall responses to antigen challenge[37] and that T_{CM} subset has superior antitumor abilities compared with T_{EM} subset,[38] we hypothesized that the former subset might rapidly migrate to the injection site of STC to confer antitumor effects. Indeed, we succeeded to demonstrate that the KO/WGM mice-derived memory Th subset had significantly stronger antitumor efficacy than the effector Th subset from the results of ACT therapy (Figure 6C).
6. We showed that the defective LTB4/BLT1 signaling in GM-CSF-triggered antitumor immunity skewed Th2 predominance in late phase (Figure 5B) and that ACT of splenic Th17 cells harvested from KO/WGM mice elicited stronger antitumor effects against WEHI3B challenge than those from WT/WGM mice (Figure 5C). Our results are compatible with the previous reports showing that memory Th2 cells had a potent antitumor immunity through IL-4–activated NK cells[39] and that the Th17 subset was decisive for yielding immunologic responses together with effector cytotoxic T lymphocytes.[40] These findings indicate that the

absence of LTB4/BLT1 signaling facilitates Th2 and Th17 polarization with antitumor phenotype, although the significance of Th2 and Th17 cells in tumor immunology is still controversial.[41,42] As frequency of multifunctional $CD4^+$ T cells simultaneously producing IFN-γ, IL-2, and TNF-α is recognized as a sensitive immune correlate for the optimized effector function against antigens,[43] we assessed the influence of the defective LTB4/BLT1 signaling on phenotypic profiles of $CD4^+$ T-cell multifunctionality. There was, however, no significant difference in frequency of each single-, or double-, or triple-cytokine producing $CD4^+$ T subset between WT/WGM and KO/WGM mice (supplemental Figure 4).

7. The absence of LTB4/BLT1 in GM-CSF–induced immunity systemically decreased production levels of the immune-regulatory cytokines in the tumor microenvironment (Figure 2I) and the infiltrated immune-regulatory $CD4^+$ T subsets in lymphoid tissue (Figure 5D-E), probably converting the immunosuppressive milieu to one that helps both generation and maintenance of memory T cells. Although other researchers showed that LTB4 plus IL-2 could generate $CD8^+$ suppressor thymocytes involved in tolerance to self-antigens,[44] there have never been relevant data delineating relationship between arachidonic-acid–derived lipid mediator, such as pro-inflammatory leukotrienes and regulatory T cell-mediated immune tolerance. Thereby, our findings could offer a hint to attenuate tumor-driven immune tolerance via the inhibition of the LTB4/ BLT1 signaling.
8. Finally, our results from in vivo depletion assays unraveled that $CD4^+$ T cells in KO/WGM mice played a predominant role in providing persistent antitumor immunity, in coordination with NK cells and $CD8^+$ T cells (Figure 6A-B), which are compatible with the previous findings that $CD4^+$ T cells are essential in the control of tumor growth through the cooperation with macrophages and cytotoxic T lymphocytes.[4,45,46] When we consider to further clarify the molecular crosstalk between LTB4 and GM-CSF signaling pathways, it will be of importance to focus on our findings that the absence of the LTB4/BLT1 axis had positive impact mainly on $CD4^+$ helper T cell-mediated adaptive immunity as evidenced by MLR assay and ACT experiments, as well as innate immunity. This novel insight that potent memory $CD4^+$ T cells in GM-CSF–triggered immunity can be retained in devoid of LTB4/BLT1signaling allows us to expect that blocking LTB4/BLT1signaling using corresponding antagonists or inhibitors may be a promising strategy to improve the therapeutic effects of GM-CSF–based tumor vaccines in clinical settings by shaping a favorable immunologic memory.

With regard to another receptor BLT2 for LTB4, it requires very high concentrations of LTB4 for its activation[47] and has been well accepted to be a receptor for 12-HHT.[48] Accordingly, it is now thought that BLT2 does not mediate any functions of LTB4 in the absence of BLT1 in vivo. We therefore disregarded the impact of BLT2 on the results of our experiments.

Intriguingly, in terms of sexual difference, the mechanism in which a superior antitumor immunity induced by WGM cells was manifested in WT female mice compared with WT male (Table 1) could possibly be explained by the following WT regulatory T cells from female mice expressing significantly lower B7-H1, a coinhibitory signaling molecule that can suppress antitumor immunity[49] and possess a more efficient phagocytic ability by resident macrophages,[50] compared with those from male mice.

In conclusion, we demonstrated that, even long after the tumor rejection, the defective LTB4/BLT1 axis facilitates effective generation of long-lasting memory $CD4^+$ T cell-dependent antitumor immunity through its positive impacts on innate and adaptive immunologic responses induced by GM-CSF.

Acknowledgments

The authors thank Dr Kazuko Saeki and Dr Toshiaki Okuno (Kyushu University) for their technical supports.

This work was supported in part by the Japan Society for the Promotion of Science (Grant-in-Aid for Young Scientists 23790446) and the Ministry of Education, Culture, Sports, Science and Technology, Japan (Grant-in-Aid for Scientific Research on Priority Areas "Cancer" 17016053).

Authorship

Contribution: Y.Y., H.I., and K. Tani designed the study and wrote manuscript; Y.Y., H.I., Y.M., C.S., and H.N. executed the experiments; Y.Y. analyzed all data; Y.Y., H.I., T.Y., and K. Tani interpreted the results of experiments; Y.Y., H.N., A.W., and F.S. contributed in the backcross and preparation of mice; and all authors discussed the results and helped conduct experiments.

Conflict-of-interest disclosure: The authors declare no competing financial interests.

Correspondence: Kenzaburo Tani, Department of Molecular Genetics, Medical Institute of Bioregulation, Kyushu University, 3-1-1, Maidashi, Higashi-ku, Fukuoka, Japan 812-8582; e-mail: taniken@bioreg.kyushu-u.ac.jp.

References

1. Jinushi M, Tahara H. Cytokine gene-mediated immunotherapy: current status and future perspectives. *Cancer Sci.* 2009;100(8):1389-1396.
2. Tani K, Azuma M, Nakazaki Y, et al. Phase I study of autologous tumor vaccines transduced with the GM-CSF gene in four patients with stage IV renal cell cancer in Japan: clinical and immunological findings. *Mol Ther.* 2004;10(4): 799-816.
3. Dranoff G. GM-CSF-based cancer vaccines. *Immunol Rev.* 2002;188:147-154.
4. Dranoff G, Jaffee E, Lazenby A, et al. Vaccination with irradiated tumor cells engineered to secrete murine granulocyte-macrophage colony-stimulating factor stimulates potent, specific, and long-lasting anti-tumor immunity. *Proc Natl Acad Sci U S A.* 1993;90(8):3539-3543.
5. Inoue H, Iga M, Nabeta H, et al. Non-transmissible Sendai virus encoding granulocyte macrophage colony-stimulating factor is a novel and potent vector system for producing autologous tumor vaccines. *Cancer Sci.* 2008;99(11):2315-2326.
6. Salgia R, Lynch T, Skarin A, et al. Vaccination with irradiated autologous tumor cells engineered to secrete granulocyte-macrophage colony-stimulating factor augments antitumor immunity in some patients with metastatic non-small-cell lung carcinoma. *J Clin Oncol.* 2003;21(4):624-630.
7. Ho VT, Vanneman M, Kim H, et al. Biologic activity of irradiated, autologous, GM-CSF-secreting leukemia cell vaccines early after allogeneic stem cell transplantation. *Proc Natl Acad Sci U S A.* 2009;106(37):15825-15830.
8. Nakazaki Y, Hase H, Inoue H, et al. Serial analysis of gene expression in progressing and regressing mouse tumors implicates the involvement of RANTES and TARC in antitumor immune responses. *Mol Ther.* 2006;14(4):599-606.
9. Simmons AD, Li B, Gonzalez-Edick M, et al. GM-CSF-secreting cancer immunotherapies: preclinical analysis of the mechanism of action. *Cancer Immunol Immunother.* 2007;56(10):1653-1665.
10. Eager R, Nemunaitis J. GM-CSF gene-transduced tumor vaccines. *Mol Ther.* 2005;12(1):18-27.

11. Lewis RA, Austen KF, Soberman RJ. Leukotrienes and other products of the 5-lipoxygenase pathway: biochemistry and relation to pathobiology in human diseases. *N Engl J Med.* 1990; 323(10):645-655.
12. Naccache PH, Sha'afi RI. Arachidonic acid, leukotriene B4, and neutrophil activation. *Ann N Y Acad Sci.* 1983;414:125-139.
13. Del Prete A, Shao WH, Mitola S, Santoro G, Sozzani S, Haribabu B. Regulation of dendritic cell migration and adaptive immune response by leukotriene B4 receptors: a role for LTB4 in up-regulation of CCR7 expression and function. *Blood.* 2007;109(2):626-631.
14. Yokomizo T, Izumi T, Chang K, Takuwa Y, Shimizu T. A G-protein-coupled receptor for leukotriene B4 that mediates chemotaxis. *Nature.* 1997;387(6633):620-624.
15. Griffin JD, Cannistra SA, Sullivan R, Demetri GD, Ernst TJ, Kanakura Y. The biology of GM-CSF: regulation of production and interaction with its receptor. *Int J Cell Cloning.* 1990;Suppl 1:35-44.
16. Miller G, Pillarisetty VG, Shah AB, Lahrs S, Xing Z, DeMatteo RP. Endogenous granulocyte-macrophage colony-stimulating factor overexpression in vivo results in the long-term recruitment of a distinct dendritic cell population with enhanced immunostimulatory function. *J Immunol.* 2002;169(6):2875-2885.
17. Terawaki K, Yokomizo T, Nagase T, et al. Absence of leukotriene B4 receptor 1 confers resistance to airway hyperresponsiveness and Th2-type immune responses. *J Immunol.* 2005; 175(7):4217-4225.
18. Nakazaki Y, Tani K, Lin ZT, et al. Vaccine effect of granulocyte-macrophage colony-stimulating factor or CD80 gene-transduced murine hematopoietic tumor cells and their cooperative enhancement of antitumor immunity. *Gene Ther.* 1998; 5(10):1355-1362.
19. Kruisbeek AM. In vivo depletion of CD4- and CD8-specific T cells. *Curr Protoc Immunol.* 1991; Chapter 4:Unit 4 1.
20. Inoue H, Iga M, Xin M, et al. TARC and RANTES enhance antitumor immunity induced by the GM-CSF-transduced tumor vaccine in a mouse tumor model. *Cancer Immunol Immunother.* 2008;57(9): 1399-1411.
21. Nurieva R, Yang XO, Chung Y, Dong C. Cutting edge: in vitro generated Th17 cells maintain their cytokine expression program in normal but not lymphopenic hosts. *J Immunol.* 2009;182(5): 2565-2568.
22. Koga Y, Matsuzaki A, Suminoe A, Hattori H, Hara T. Neutrophil-derived TNF-related apoptosis-inducing ligand (TRAIL): a novel mechanism of antitumor effect by neutrophils. *Cancer Res.* 2004;64(3):1037-1043.
23. Di Carlo E, Forni G, Lollini P, Colombo MP, Modesti A, Musiani P. The intriguing role of polymorphonuclear neutrophils in antitumor reactions. *Blood.* 2001;97(2):339-345.
24. Tong WG, Ding XZ, Hennig R, et al. Leukotriene B4 receptor antagonist LY293111 inhibits proliferation and induces apoptosis in human pancreatic cancer cells. *Clin Cancer Res.* 2002;8(10): 3232-3242.
25. Ihara A, Wada K, Yoneda M, Fujisawa N, Takahashi H, Nakajima A. Blockade of leukotriene B4 signaling pathway induces apoptosis and suppresses cell proliferation in colon cancer. *J Pharmacol Sci.* 2007;103(1):24-32.
26. Mach N, Gillessen S, Wilson SB, Sheehan C, Mihm M, Dranoff G. Differences in dendritic cells stimulated in vivo by tumors engineered to secrete granulocyte-macrophage colony-stimulating factor or Flt3-ligand. *Cancer Res.* 2000;60(12): 3239-3246.
27. Serafini P, Carbley R, Noonan KA, Tan G, Bronte V, Borrello I. High-dose granulocyte-macrophage colony-stimulating factor-producing vaccines impair the immune response through the recruitment of myeloid suppressor cells. *Cancer Res.* 2004;64(17): 6337-6343.
28. Hung K, Hayashi R, Lafond-Walker A, Lowenstein C, Pardoll D, Levitsky H. The central role of CD4(+) T cells in the antitumor immune response. *J Exp Med.* 1998;188(12):2357-2368.
29. Shimizu J, Yamazaki S, Takahashi T, Ishida Y, Sakaguchi S. Stimulation of CD25(+)CD4(+) regulatory T cells through GITR breaks immunological self-tolerance. *Nat Immunol.* 2002;3(2): 135-142.
30. Nocentini G, Riccardi C. GITR: a multifaceted regulator of immunity belonging to the tumor necrosis factor receptor superfamily. *Eur J Immunol.* 2005;35(4):1016-1022.
31. Veiga-Fernandes H, Walter U, Bourgeois C, McLean A, Rocha B. Response of naive and memory CD8+ T cells to antigen stimulation in vivo. *Nat Immunol.* 2000;1(1):47-53.
32. Hoque A, Lippman SM, Wu TT, et al. Increased 5-lipoxygenase expression and induction of apoptosis by its inhibitors in esophageal cancer: a potential target for prevention. *Carcinogenesis.* 2005;26(4):785-791.
33. Avis IM, Jett M, Boyle T, et al. Growth control of lung cancer by interruption of 5-lipoxygenase-mediated growth factor signaling. *J Clin Invest.* 1996;97(3):806-813.
34. Yokomizo T. Leukotriene B4 receptors: novel roles in immunological regulations. *Adv Enzyme Regul.* 2011;51(1):59-64.
35. Alter G, Malenfant JM, Altfeld M. CD107a as a functional marker for the identification of natural killer cell activity. *J Immunol Methods.* 2004; 294(1):15-22.
36. Toda A, Terawaki K, Yamazaki S, Saeki K, Shimizu T, Yokomizo T. Attenuated Th1 induction by dendritic cells from mice deficient in the leukotriene B4 receptor 1. *Biochimie.* 2010;92(6):682-691.
37. Kaech SM, Wherry EJ, Ahmed R. Effector and memory T-cell differentiation: implications for vaccine development. *Nat Rev Immunol.* 2002;2(4): 251-262.
38. Fearon DT, Manders P, Wagner SD. Arrested differentiation, the self-renewing memory lymphocyte, and vaccination. *Science.* 2001;293(5528): 248-250.
39. Kitajima M, Ito T, Tumes DJ, et al. Memory type 2 helper T cells induce long-lasting antitumor immunity by activating natural killer cells. *Cancer Res.* 2011;71(14):4790-4798.
40. Kryczek I, Banerjee M, Cheng P, et al. Phenotype, distribution, generation, and functional and clinical relevance of Th17 cells in the human tumor environments. *Blood.* 2009;114(6):1141-1149.
41. Muranski P, Restifo NP. Does IL-17 promote tumor growth? *Blood.* 2009;114(2):231-232.
42. Bronte V. Th17 and cancer: friends or foes? *Blood.* 2008;112(2):214.
43. Seder RA, Darrah PA, Roederer M. T-cell quality in memory and protection: implications for vaccine design. *Nat Rev Immunol.* 2008;8(4):247-258.
44. Gualde N, Cogny van Weydevelt F, Buffiere F, Jauberteau MO, Daculsi R, Vaillier D. Influence of LTB4 on CD4−, CD8− thymocytes: evidence that LTB4 plus IL-2 generate CD8+ suppressor thymocytes involved in tolerance to self. Effect of LTB4 and IL-2 on double negative thymocytes. *Thymus.* 1991;18(2):111-128.
45. Corthay A, Skovseth DK, Lundin KU, et al. Primary antitumor immune response mediated by CD4+ T cells. *Immunity.* 2005;22(3):371-383.
46. Qin Z, Blankenstein T. CD4+ T cell–mediated tumor rejection involves inhibition of angiogenesis that is dependent on IFN gamma receptor expression by nonhematopoietic cells. *Immunity.* 2000;12(6):677-686.
47. Yokomizo T, Kato K, Terawaki K, Izumi T, Shimizu T. A second leukotriene B(4) receptor, BLT2: a new therapeutic target in inflammation and immunological disorders. *J Exp Med.* 2000;192(3):421-432.
48. Okuno T, Iizuka Y, Okazaki H, Yokomizo T, Taguchi R, Shimizu T. 12(S)-Hydroxyheptadeca-5Z, 8E, 10E-trienoic acid is a natural ligand for leukotriene B4 receptor 2. *J Exp Med.* 2008;205(4):759-766.
49. Lin PY, Sun L, Thibodeaux SR, et al. B7-H1-dependent sex-related differences in tumor immunity and immunotherapy responses. *J Immunol.* 2010;185(5):2747-2753.
50. Scotland RS, Stables MJ, Madalli S, Watson P, Gilroy DW. Sex differences in resident immune cell phenotype underlie more efficient acute inflammatory responses in female mice. *Blood.* 2011;118(22):5918-5927.

PLOS ONE

The CD3 versus CD7 Plot in Multicolor Flow Cytometry Reflects Progression of Disease Stage in Patients Infected with HTLV-I

Seiichiro Kobayashi[1], Yamin Tian[1,2], Nobuhiro Ohno[3], Koichiro Yuji[3], Tomohiro Ishigaki[4], Masamichi Isobe[3], Mayuko Tsuda[3], Naoki Oyaizu[5], Eri Watanabe[4], Nobukazu Watanabe[4], Kenzaburo Tani[2], Arinobu Tojo[1,3], Kaoru Uchimaru[3]*

1 Division of Molecular Therapy, Institute of Medical Science, The University of Tokyo, Tokyo, Japan, **2** Department of Molecular Genetics, Medical Institute of Bioregulation, Kyushu University, Fukuoka, Japan, **3** Department of Hematology/Oncology, Research Hospital, Institute of Medical Science, The University of Tokyo, Tokyo, Japan, **4** Laboratory of Diagnostic Medicine, Division of Stem Cell Therapy, Institute of Medical Science, The University of Tokyo, Tokyo, Japan, **5** Clinical Laboratory, Research Hospital, Institute of Medical Science, The University of Tokyo, Tokyo, Japan

Abstract

Purpose: In a recent study to purify adult T-cell leukemia-lymphoma (ATL) cells from acute-type patients by flow cytometry, three subpopulations were observed in a CD3 versus CD7 plot (H: $CD3^{high}CD7^{high}$; D: $CD3^{dim}CD7^{dim}$; L: $CD3^{dim}CD7^{low}$). The majority of leukemia cells were enriched in the L subpopulation and the same clone was included in the D and L subpopulations, suggesting clonal evolution. In this study, we analyzed patients with indolent-type ATL and human T-cell leukemia virus type I (HTLV-I) asymptomatic carriers (ACs) to see whether the CD3 versus CD7 profile reflected progression in the properties of HTLV-I-infected cells.

Experimental Design: Using peripheral blood mononuclear cells from patient samples, we performed multi-color flow cytometry. Cells that underwent fluorescence-activated cell sorting were subjected to molecular analyses, including inverse long PCR.

Results: In the D(%) versus L(%) plot, patient data could largely be categorized into three groups (Group 1: AC; Group 2: smoldering- and chronic-type ATL; and Group 3: acute-type ATL). Some exceptions, however, were noted (*e.g.*, ACs in Group 2). In the follow-up of some patients, clinical disease progression correlated well with the CD3 versus CD7 profile. In clonality analysis, we clearly detected a major clone in the D and L subpopulations in ATL cases and, intriguingly, in some ACs in Group 2.

Conclusion: We propose that the CD3 versus CD7 plot reflects progression of disease stage in patients infected with HTLV-I. The CD3 versus CD7 profile will be a new indicator, along with high proviral load, for HTLV-I ACs in forecasting disease progression.

Citation: Kobayashi S, Tian Y, Ohno N, Yuji K, Ishigaki T, et al. (2013) The CD3 versus CD7 Plot in Multicolor Flow Cytometry Reflects Progression of Disease Stage in Patients Infected with HTLV-I. PLoS ONE 8(1): e53728. doi:10.1371/journal.pone.0053728

Editor: Jean-Pierre Vartanian, Institut Pasteur, France

Received August 31, 2012; **Accepted** December 4, 2012; **Published** January 22, 2013

Funding: This study was supported by the Ministry of Education, Culture, Sports, Science and Technology, Japan. The funders had no role in study design, data collection and analysis, decision to publish, or preparation of the manuscript.

Competing Interests: The authors have declared that no competing interests exist.

* E-mail: uchimaru@ims.u-tokyo.ac.jp

Introduction

Human T-cell leukemia virus type I (HTLV-I) is the agent that causes HTLV-I-associated diseases, such as adult T-cell leukemia-lymphoma (ATL), HTLV-I-associated myelopathy/tropical spastic paraparesis (HAM/TSP), and HTLV-I uveitis (HU) [1–3]. Approximately 10–20 million people are infected with the HTLV-I virus worldwide [4]. The lifetime risk of developing ATL is estimated to be approximately 2.5–5% [5,6]. ATL includes a spectrum of diseases that are referred to as smoldering-, chronic-, lymphoma-, and acute-type [7,8]. The chronic and smoldering types of ATL are considered indolent and are usually managed with watchful waiting until the disease progresses to aggressive (lymphoma- or acute-type) ATL [9]. Because the prognosis of ATL is poor with current treatment strategies, factors to forecast progression to ATL from asymptomatic carriers (ACs) have been researched [10–13] in the hope that they will be useful for preventive therapy under development in the early malignant stage.

Various cellular dysfunctions induced by viral genes (*e.g.*, tax and HBZ), genetic and epigenetic alterations, and the host immune system are considered to cooperatively contribute to leukemogenesis in ATL [14–16]. However, the complex mechanism may hinder determination of a clear mechanism of the pathology and make discovery of risk factors difficult. In a prospective nationwide study in Japan, high proviral load (VL,

Table 1. Clinical profile of patients infected with HTLV-I and normal controls.

Clinical sutype	Number of cases	Male	Female	Age (range)	WBC(/μl) (range)	Lymphocytes(%) (range)	Abnormal lymphocytes(%) (range)
HTLV-1 AC	40	12	28	49.9	5525	35.9	0.9
				(28–70)	(2680–10360)	(22.4–59.5)	(0.0–4.4)
Smoldering	7	4	3	55.3	5944	32.5	5.8
				(43–77)	(3680–8710)	(13.4–47.5)	(0.7–16.5)
Chronic	7	4	3	52.7	9180	45.8	9.2
				(37–60)	(4070–12790)	(35.0–61.5)	(3.4–12.7)
Acute	13	4	9	58.8	15328	16.3	40.3
				(42–74)	(4450–41480)	(1.7–50.5)	(3.0–89.6)
Normal controls	10	6	4	47.4	ND	ND	ND
				(27–66)			

WBC: white blood cells (normal range, 3500–9100/μl).
AC: asymptomatic carrier.
ND: analysis were not performed.
Average of age, WBC, lymphocytes (%) and abnormal lymphocytes (%) are shown.
The proportion of abonormal lymphocytes in peripheral blood WBCs was evaluated by morphological exmanination.
doi:10.1371/journal.pone.0053728.t001

over 4.17 copies/100 peripheral blood mononuclear cells) was found to be a major risk factor for HTLV-I AC developing into ATL [13]. Although VL indicates the proportion of HTLV-I-infected cells, it does not indicate size or degree of malignant progression in each clone; *i.e.*, it does not directly indicate progression of disease stage in HTLV-I infection. Moreover, the majority of ACs with high VL remained intact during the study period, indicating that a more accurate indicator of progression is needed.

In our recent study to purify monoclonal ATL cells from acute-type patients by flow cytometry, three subpopulations were observed in a CD3 versus CD7 plot of $CD4^+$ cells (H: $CD3^{high}CD7^{high}$, D: $CD3^{dim}CD7^{dim}$, L: $CD3^{dim}CD7^{low}$), and the majority of ATL cells were enriched in the L subpopulation [17]. Clonality analyses revealed that the D and L subpopulations contained the same clone, suggesting clonal evolution of HTLV-I-infected cells to ATL cells. From these findings, we speculated that the CD3 versus CD7 profile may reflect disease progression in HTLV-I infection. In this study, the CD3 versus CD7 profile by flow cytometry, combined with molecular (clonality and proviral load) characterizations, were analyzed in patients with various clinical subtypes (HTLV-I AC, and indolent and aggressive ATL). We found that the CD3 versus CD7 profile reflected disease progression of HTLV-I-infected cells to ATL cells. We also discuss the significance of this analysis as a novel risk indicator for HTLV-I ACs in forecasting progression to ATL.

Materials and Methods

Cell lines and patient samples

TL-Om1, an HTLV-I-infected cell line, established Dr. Hinuma's laboratory [18], was provided by Dr. Toshiki Watanabe (The University of Tokyo, Tokyo, Japan) and was cultured in RPMI-1640 medium containing 10% fetal bovine serum. Peripheral blood samples were collected from inpatients and outpatients at our hospital from August 2009 to November 2011. All patients with ATL were categorized according to Shimoyama's criteria [7,8]. Patients with various complications, such as autoimmune disorder and systemic infections, were excluded. Lymphoma-type patients were excluded because ATL cells are not considered to exist in peripheral blood of this clinical subtype. In patients with ATL receiving chemotherapy, blood samples were collected before treatment or during the recovery phase between chemotherapy sessions. Samples collected from 10 healthy volunteers (mean age: 47.4 years; range: 27–66 years) were used as normal controls.

The present study was approved by the research ethics committee of the institute of medical science, the university of Tokyo. Subjects provided written informed consent.

Flow cytometry and cell sorting

Peripheral blood mononuclear cells (PBMCs) were isolated from heparin-treated whole blood by density gradient centrifugation, as described previously [17]. Cells were stained using a combination of phycoerythrin (PE)-CD7, APC-Cy7-CD3, Pacific Blue-CD4, and Pacific Orange-CD14. Pacific Orange-CD14 was purchased from Caltag-Invitrogen (Carlsbad, CA). All other antibodies were obtained from BD BioSciences (San Jose, CA). Propidium iodide (PI; Sigma, St. Louis, MO) was added to the samples to stain dead cells immediately prior to flow cytometry. A BD FACS Aria instrument (BD Immunocytometry Systems, San Jose, CA) was used for all multicolor flow cytometry and cell sorting. Data were analyzed using the FlowJo software (Treestar, San Carlos, CA).

Quantification of HTLV-I proviral load by real-time quantitative polymerase chain reaction (PCR)

The HTLV-I proviral load in FACS-sorted PBMCs was quantified by real-time quantitative polymerase chain reaction (PCR; TaqMan method) using the ABI Prism 7000 sequence detection system (Applied Biosystems, Foster City, CA) as described previously [13,17]. Briefly, 50 ng of genomic DNA was extracted from human PBMCs using a QIAamp DNA blood Micro kit (Qiagen, Hilden, Germany). Triplicate samples of the DNA were amplified. Each PCR mixture, containing an HTLV-I pX region-specific primer pair at 0.1 μM (forward primer 5′-CGGATACCCAGTCTACGTGTT-3′ and reverse primer 5′-

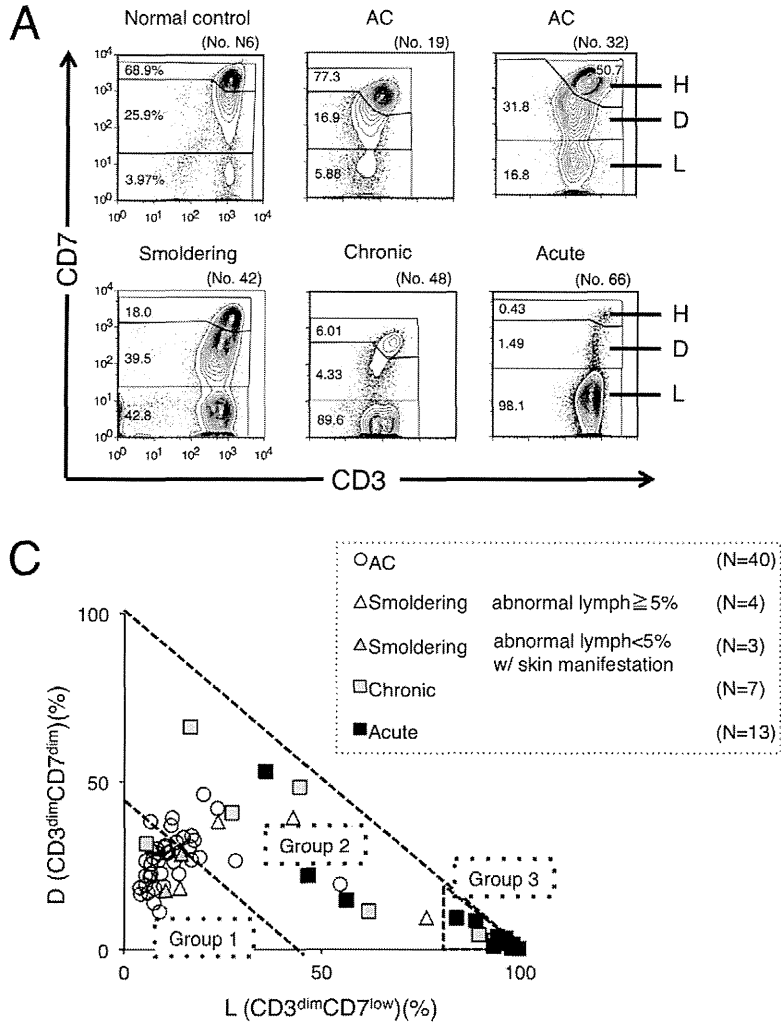

Figure 1. CD3 versus CD7 plots in flow cytometric analysis of patients who are asymptomatic HTLV-I carriers (ACs) and have various clinical subtypes of adult T-cell leukemia-lymphoma (ATL) suggest disease progression in HTLV-I infection. (A) Flow cytometric profile of an AC, various clinical subtypes of ATL (smoldering, chronic, and acute), and a normal control. Representative cases of CD3 versus CD7 plots in $CD4^+$ cells are shown. (B) A two-dimensional plot of AC cases showing the percentage of the D and L subpopulations by flow cytometry. AC cases were divided into two groups according to HTLV-I VL (greater or less than 4%). The border line (45% of D+L subpopulations) between Group 1 and 2 was set based on proviral load (VL). All AC cases with less than 4% VL were included in Group 1. All AC cases included in Group 2 had greater than 4% VL. VL<4%: n = 21; VL>4%: n = 19. All VL data in this figure were provided from the database of the Joint Study on Predisposing Factors of ATL Development (JSPFAD). (C) A two-dimensional plot of all patients showing the percentage of the D and L subpopulations. The smoldering type was divided into two categories: smoldering type with greater than 5% abnormal lymphocytes and smoldering type with less than 5% abnormal lymphocytes with skin manifestation. The two diagonal dotted lines indicate 45% and 100% of D+L subpopulations (*i.e.*, 55% and 0% of the H subpopulation). Data were categorized into three groups.
doi:10.1371/journal.pone.0053728.g001

CAGTAGGGCGTGACGATGTA-3′), FAM-labeled probe at 0.1 μM (5′- CTGTGTACAAGGCGACTGGTGCC-3′), and 1× TaqMan Universal PCR master mix (Applied Biosystems), was subjected to 50 cycles of denaturation (95°C, 15 seconds) and annealing to extension (60°C, 1 minute), following an initial Taq polymerase activation step (95°C, 10 minutes). The RNase P control reagent (Applied Biosystems) was used as an internal control for calculating the input cell number (using VIC reporter dye). DNAs extracted from TL-Om1 and normal human PBMCs were used as positive and negative controls, respectively. The HTLV-I proviral load (%) was calculated as the copy number of the pX region per input cell number. To correct the deviation of data acquired in each experiment, data from TL-Om1 (positive control) were adjusted to 100%, and the sample data were corrected accordingly by a proportional calculation.

Inverse long PCR

For clonality analysis, inverse long PCR was performed [17]. First, 1 μg of genomic DNA extracted from the FACS-sorted cells was digested with *Eco*RI and *Pst*I at 37°C overnight. Purification of DNA fragments was performed using a QIAEX2 gel extraction kit (Qiagen). The purified DNA was self-ligated with T4 DNA ligase (Takara Bio, Otsu, Japan) at 16°C overnight. The circular DNA obtained from the *Eco*RI digestion fragment was then digested

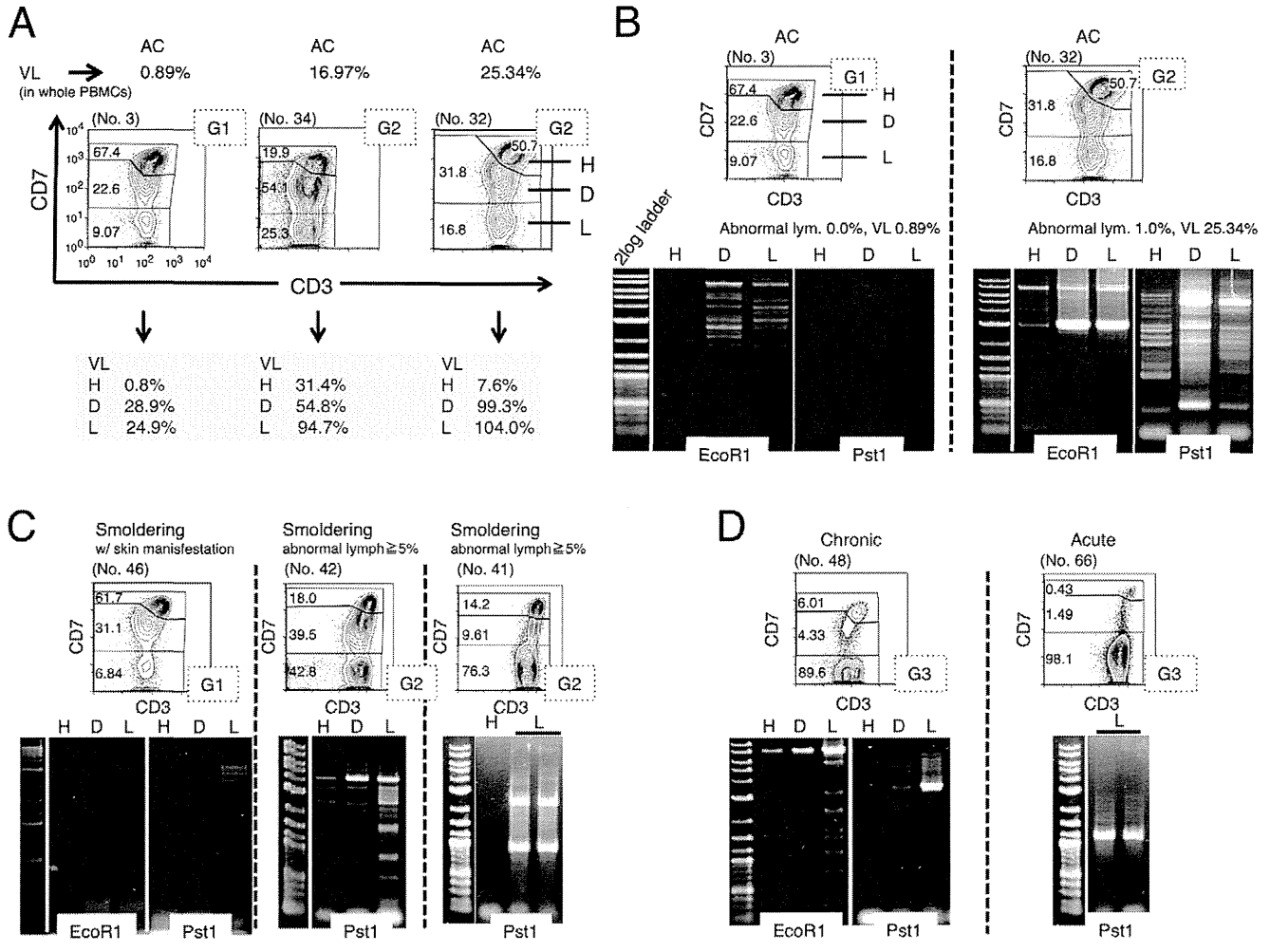

Figure 2. HTLV-I proviral load (VL) and clonality in each subpopulation, based on the CD3 versus CD7 plot. (A) The three subpopulations (H, D, L) based on the CD3 versus CD7 plot were subjected to fluorescence-activated cell sorting (FACS) and VL analysis. Three representative cases are shown. G1 or G2 in the dotted box indicates Group 1 or Group 2, categorized by the percentage of the D and L subpopulations, respectively. (B)–(D) Analysis of clonality in the three subpopulations based on the CD3 versus CD7 plot. Genomic DNA was extracted from FACS-sorted cells of each subpopulation and subjected to inverse long polymerase chain reaction (PCR). Representative data of two cases of AC (B), three cases of smoldering type, including one with skin manifestations (C), and cases of a chronic type and an acute type (D) are shown. PCR was performed in duplicate (black bars) in cases when a sufficient amount of DNA was obtained.
doi:10.1371/journal.pone.0053728.g002

with *Mlu*I, which cuts the pX region of the HTLV-I genome and prevents amplification of the viral genome. Inverse long PCR was performed using Takara LA *Taq* polymerase (Takara Bio). For the *Eco*RI-treated template, the forward primer was 5′-TGCCTGACCCTGCTTGCTCAACTCTACGTCTTTG-3′ and the reverse primer was 5′-AGTCTGGGCCCT-GACCTTTTCAGACTTCTGTTTC-3′. For the *Pst*I-treated group, the forward primer was 5′-CAGCCCATTCTATAG-CACTCTCCAGGAGAG-3′ and the reverse primer was 5′-CAGTCTCCAAACACGTAGACTGGGTATCCG-3. Each 50-μL reaction mixture contained 0.4 mM of each dNTP, 25 mM $MgCl_2$, 10× LA PCR buffer II containing 20 mM Tris-HCl and 100 mM KCl, 0.5 mM of each primer, 2.5 U LA *Taq* polymerase, and 50 ng of the processed genomic DNA. The reaction mixture was subjected to 35 cycles of denaturation (94°C, 30 seconds) and annealing to extension (68°C, 8 minutes). Following PCR, the products were subjected to electrophoresis on 0.8% agarose gels. In samples from which a sufficient amount of DNA was extracted, PCRs were performed in duplicate.

Results

CD3 versus CD7 profile in flow cytometry in various clinical subtypes of patients infected with HTLV-I

The clinical profiles of the 77 cases analyzed in this study are shown in Table 1. According to the gating procedure, as shown in Figure S1 [17], we constructed a CD3 versus CD7 plot of $CD4^+$ cells in PBMCs of various clinical subtypes from patients infected with HTLV-I and normal controls. The three subpopulations ($CD3^{high}CD7^{high}$, $CD3^{dim}CD7^{dim}$, and $CD3^{dim}CD7^{low}$) observed are referred to as the H, D, and L subpopulations, respectively. Representative results for each clinical subtype of HTLV-I infection are shown in Figure 1A. Regarding the data for an acute-type patient (no. 66), the dominant population was the L subpopulation, in which we previously demonstrated that monoclonal ATL cells are enriched [17]. Regarding the AC (no. 19), the CD3 versus CD7 profile was close to that of the normal control, although in some AC cases, such as no. 32, the profile differed from that of the normal control, because in contrast to case no. 19,

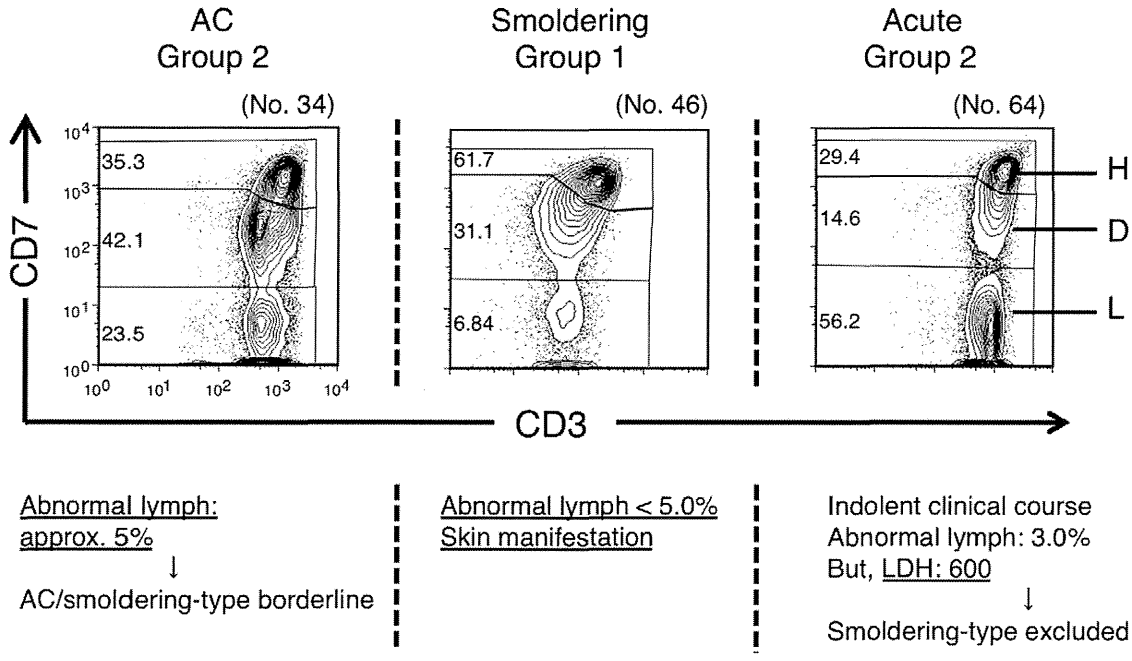

Figure 3. Study of exceptional cases categorized by proportion of the $CD3^{dim}CD7^{dim}$ (D) and $CD3^{dim}CD7^{low}$ (L) subpopulations. Left: An HTLV-I AC patient who was categorized in Group 2 in the D(%) versus L(%) plot. Middle: A patient with smoldering-type ATL who was categorized in Group 1. Right: A patient with acute-type ATL who was categorized in Group 2.
doi:10.1371/journal.pone.0053728.g003

these cases had increased D and L subpopulations. Regarding the data for indolent-type disease (smoldering and chronic), increases in the D and L subpopulations were intermediate between ACs and patients with acute-type disease. These representative flow cytometric data suggest that continuity in the CD3 versus CD7 profile seemed to exist among the various clinical subtypes of patients infected with HTLV-I.

The proportions of D and L subpopulations in all AC cases analyzed are shown in Figure 1B. Because the high HTLV-I proviral load (VL) in whole PBMCs, a VL of >4%, was reported to be a major risk indicator for progression to ATL [13], a border line was set based on VL. Group 1, the area under the diagonal line (D+L = 45%), included all AC cases with VLs of <4%. ACs with VLs of >4% were distributed between Groups 1 and 2. The proportions of D and L subpopulations in normal controls are shown in Figure S2. In this plot, all data for normal controls were distributed in Group 1. Data for all clinical subtypes are shown in Figure 1C. Most data for acute-type patients were located in the area beyond 80% of the L subpopulation and we designated this area as Group 3. Group 2, which is located between Group 1 and Group 3, included the majority of indolent-type (smoldering and chronic) cases. From these results, the three groups in the D(%) versus L(%) plot seemed to represent disease stage in each case.

Proviral load and clonality in each subpopulation in the CD3 versus CD7 plot

To further characterize each subpopulation (H, D, and L) in the CD3 versus CD7 plot, cells in each subpopulation were FACS-sorted and subjected to analysis of VL to determine the percentage of HTLV-I-infected cells in each subpopulation. Results for representative cases are shown in Figure 2A. The VL in whole PBMCs of an AC (no. 3) was low (0.89%). As expected, the VL in H, the major subpopulation, was low (0.8%). However, VLs in the D and L subpopulations were considerably higher (28.9% and 24.9%, respectively), indicating that HTLV-I-infected cells are relatively concentrated in these subpopulations. In the cases with high VLs in whole PBMCs (no. 32 with 25.34%; no. 34 with 16.97%), the VLs were also higher in the D and L subpopulations, and almost all cells in the L subpopulation were HTLV-I-infected.

In HTLV-I infection, progression to ATL requires several pathological steps, including clonal expansion [15]. To further characterize the three subpopulations based on the CD3 versus CD7 plot, we analyzed clonality in each subpopulation in patients with various clinical subtypes using the inverse long PCR method. Figure 2B shows two cases of AC. In the left case (no. 3), included in Group 1 in the D(%) and L(%) plot, multiple bands suggestive of multiple small clones were detected in the three subpopulations. However, no major band suggestive of a dominant clone was observed. In the right case (no. 32), included in Group 2, inverse long PCR of the FACS-sorted subpopulations suggested that the D and L subpopulations contained a major clone (Figure 2B). The D subpopulation had bands of the same size as those of the L subpopulation, indicating that the two distinct subpopulations contained a common major clone. Eleven cases of AC were included in Group 2. All three cases analyzed by Southern blotting (whole blood samples) were positive for clonal bands (Figure S3). In Figure 2C, data for three smoldering cases are shown. In case no. 46 (left), whose only manifestation was a skin eruption with few abnormal lymphocytes (less than 5% of white blood cells) in the peripheral blood, only faint minor bands suggestive of small clones were observed. In contrast, in the other two cases (nos. 42 and 41), intense bands suggestive of major clones were observed in both the D and L subpopulations. In no. 41 (right), weak bands were not visible, which suggested the selection of dominant clones. In Figure 2D, data for a chronic-type case and an acute-type case are shown. In both cases, intense bands in the L subpopulation suggest the existence of a major clone. The series of clonality analyses indicated that a major clone became more evident and the clinical

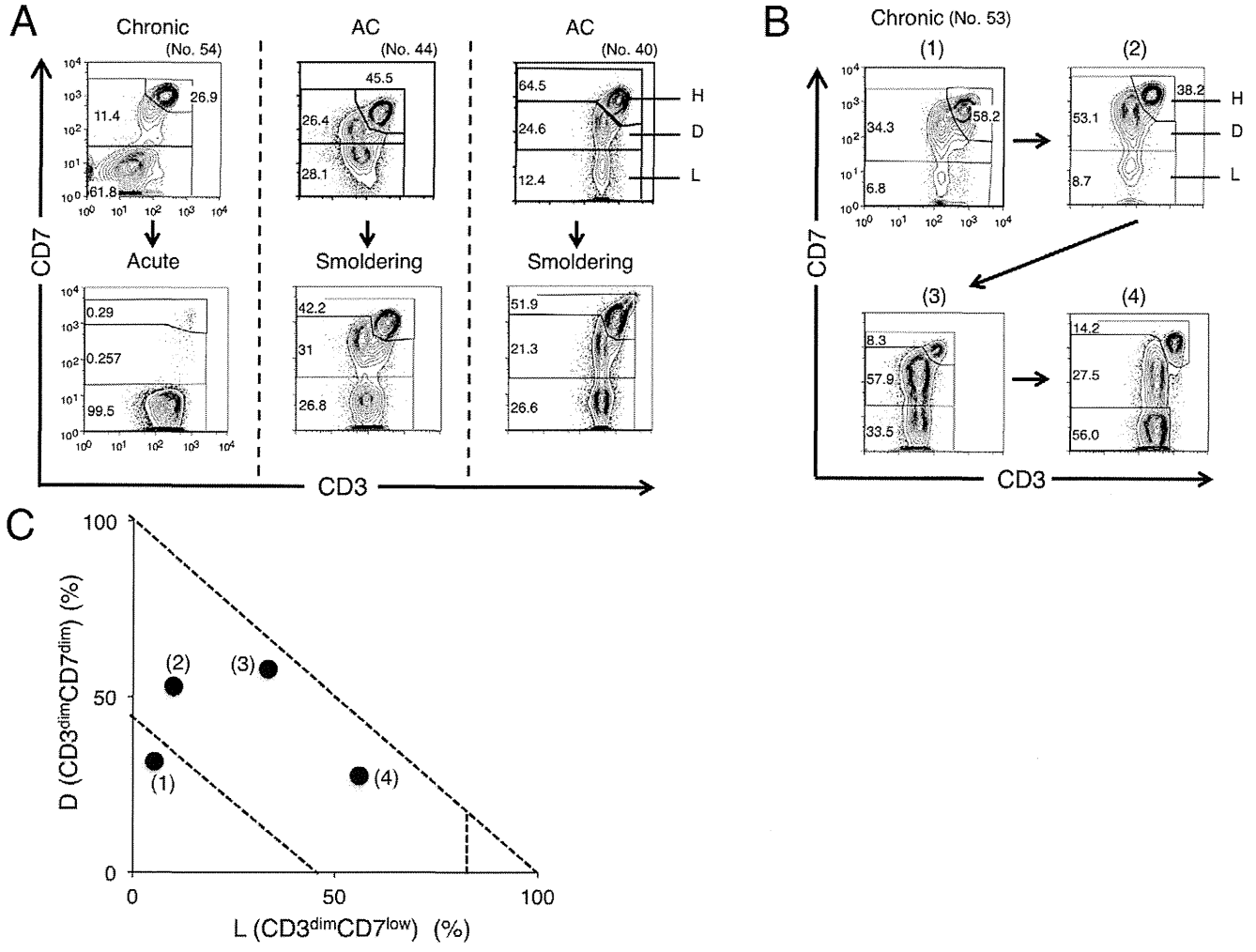

Figure 4. Alteration in the CD3 versus CD7 profile by flow cytometry in accordance with disease progression. (A) Change in the CD3 versus CD7 profile in representative cases. In all three cases shown, change in clinical data (*e.g.*, abnormal lymphocyte, LDH) resulted in progression of the clinical subtype. (B) Change in the CD3 versus CD7 profile in a time course in the case of chronic-type ATL. Clinical data are shown in Table S1. (C) Flow cytometric data in (B) are summarized in the D(%) versus L(%) plot.
doi:10.1371/journal.pone.0053728.g004

stage became more advanced as the D and L subpopulations increased.

Clinical evaluation of exceptional cases categorized by proportions of the $CD3^{dim}CD7^{dim}$ (D) and $CD3^{dim}CD7^{low}$ (L) subpopulations

As noted above, the D(%) versus L(%) plot generally represented disease stage in HTLV-I infection. However, we observed one case of chronic-type disease and three cases of smoldering-type disease in Group 1 and three cases of acute-type disease in Group 2. Furthermore, some ACs with VLs of >4% were observed in Group 2. Representative data from these apparently exceptional cases are shown in Figure 3. On the left, a case of AC (no. 34) observed in Group 2 is shown. 4.7% of lymphocytes in this blood sample were abnormal and clonality analysis by Southern blotting showed oligoclonal bands suggestive of clones of substantial size (Figure S3). These clinical data suggest that the disease stage would be around the AC/smoldering borderline. In the middle, a case of a smoldering type (no. 46) observed in Group 1 is shown. In this case, the percentage of abnormal lymphocytes in the peripheral blood was only 1%, but she had a histologically proven ATL lesion in the skin and was diagnosed with smoldering-type ATL. The other two smoldering cases categorized in Group 1 were the same as this case. These results indicate that ATL cells in these three smoldering cases infiltrated the skin, but not the peripheral blood. On the right, a case of acute-type disease categorized as Group 2 (no. 64) is shown. The clinical course of this patient was relatively indolent compared with typical acute-type disease. He had skin infiltration of ATL cells, but no lymph node swelling. However, LDH exceeded 1.5 times the upper limit of the normal range, which excludes a diagnosis of smoldering-type disease. Other acute-type cases categorized in Group 2 were diagnosed as such according to Shimoyama's criteria, but also had the same indolent clinical course as case no. 64. These cases should have been regarded as indolent ATL.

Changes in the CD3 versus CD7 profile in flow cytometry with disease progression

In several cases, we could obtain time-sequential samples (Figure 4). The patient (no. 54) shown on the left in Figure 4A progressed from chronic-type to acute-type disease. In flow cytometric analysis, decreases in the H and D subpopulations

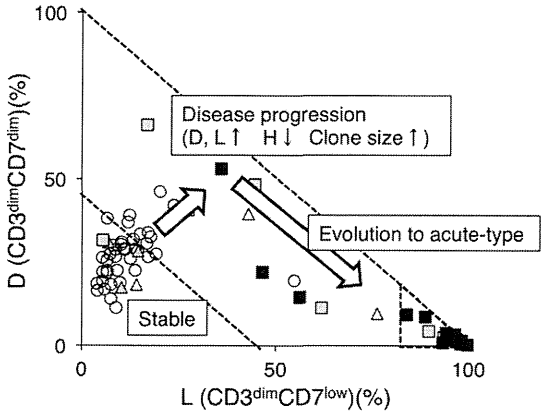

Figure 5. Summary of the study: the CD3 versus CD7 profile reflects progression of disease stage in patients infected with HTLV-I. In the percentage of D ($CD3^{dim}CD7^{dim}$) versus L ($CD3^{dim}CD7^{low}$) plot, Group 1 includes the majority of AC cases. As disease stage progresses, the CD3 versus CD7 profile then changes. With downregulation of CD3 and CD7, the D and L subpopulations increase gradually (Group 2). During this step, clones in the D and L subpopulations increase in size. Further accumulation of genetic alterations will result in rapid expansion of ATL clones—*i.e.*, evolution to acute-type ATL. In this step, the CD3 versus CD7 profile will progress from Group 2 to 3.
doi:10.1371/journal.pone.0053728.g005

and an increase in the L subpopulation were observed, indicating that disease progression correlated well with the change in the CD3 versus CD7 profile. The patients in the middle (no. 44) and on the right (no. 40) were included in Group 2 at the AC stage and later progressed to smoldering-type ATL. Although variation in the change of the flow cytometric profile was seen between these patients, the results suggest that ACs in Group 2 are at high risk of developing ATL.

The patient in Figure 4B (no. 53) was initially diagnosed with AC and later progressed to chronic-type ATL. Although the initial clinical course was stable, an increase in abnormal lymphocyte numbers was later observed, and low-dose VP-16 therapy (50 mg/day) was initiated because of hypoxemia due to lung infiltration of ATL cells. Table S1 and Figure 4C show summaries of the clinical data and the flow cytometric analyses, respectively. The flow cytometric data correlated well with disease progression.

Discussion

Findings in our previous analysis of acute-type ATL samples prompted our analysis of various clinical subtypes of patients infected with HTLV-I to examine whether the CD3 versus CD7 profile reflects the progression of oncogenesis in HTLV-I-infected cells [17]. Representative flow cytometric data shown in Figure 1A suggested that the CD3 versus CD7 profile changed during disease progression. As the disease stage progressed, the D and L subpopulations increased with concomitant decreases in the $CD3^{high}CD7^{high}$(H) subpopulation. Figure 1C, a summary of the flow cytometric data of all cases analyzed, reveals that the two-dimensional plot of the proportions of the D versus L subpopulations could divide all cases into three groups. Group 1, the area under the diagonal line, equivalent to 55% of the H subpopulation in which all normal controls were included (Figure S2), contained the majority of HTLV-I ACs. Group 3 was the area beyond 80% of the L subpopulation, and the majority of acute-type cases were included in this group. Group 2, located between Groups 1 and 3 (*i.e.*, less than 55% of the H subpopulation and 80% of the L subpopulation), included indolent-type (smoldering and chronic) cases and some AC cases. These results suggest that the CD3 versus CD7 expression profile reflects disease stage. Initially, both the D and L subpopulations gradually and simultaneously increased. However, at the clinically advanced stage, the increase in the L subpopulation was prominent. The change is considered to reflect the biological difference between the D and L subpopulations, which needs to be clarified.

In HTLV-I infection, the small clones of infected cells are considered to coexist from the AC stage [19,20]. A selected clone from the multiple small clones then grows and progresses to the malignant state, and the emergence of a dominant clone indicates disease progression in ATL [19,20]. As shown in Figure 2B–D, major bands suggesting dominant clones were evident in patients with progressed clinical subtypes or those in the advanced group in the CD3 versus CD7 profile, and major bands existed exclusively in the D and L subpopulations. These data also support the idea that increases in the D and L subpopulations correlate with the progression of disease stage. AC cases in Group 2 had high HTLV-I proviral loads (>4%; Figure 1B) and clear major bands were observed by inverse long PCR in these cases (Figure 2B, right). Sasaki *et al.* reported that two cases of HTVL-I AC with oligoclonal bands on Southern blots and high VLs (20%) had progressed to ATL by 4 and 3.5 years later [21]. The two cases may correspond to HTLV-I AC in Group 2 proposed in our study. In fact, two cases of ACs in our series that were included in Group 2 progressed to smoldering ATL (Figure 4A). AC cases in Group 2 could be regarded as advanced carriers. Our flow cytometric analysis could apparently discriminate high-risk AC cases from stable ones. Follow-up analysis of these cases is warranted to determine whether AC cases included in Group 2 progress to ATL. Flow cytometric data for these AC cases included in Group 2 (Figure 1A and 1C) were similar to those for indolent ATL cases in Group 2. These ACs in Group 2 can be considered essentially the same as smoldering ATL cases. Some of the ACs categorized according to Shimoyama's criteria should in fact be separated and regarded as a subtype together with at least some of the smoldering ATL cases.

Iwanaga *et al.* reported that high HTLV-I proviral load (>4%) in whole PBMCs was a risk factor for progression to ATL [13]. In Figure 1B, the ACs with VLs>4% were distributed between Groups 1 and 2. These findings suggest that not all ACs with high VLs are currently in an advanced stage, although they may have the potential to develop ATL in the future.

In general, the categorization by flow cytometric profile correlated well with the current classification of clinical subtypes, with some exceptional cases of acute-type and smoldering-type disease (Figure 3). The only manifestation of three smoldering cases categorized in Group 1 was skin lesions; they fell into Group 1 because they showed minimal abnormalities in peripheral blood [22]. Three acute-type ATL cases categorized in Group 2 had indolent clinical courses. A diagnosis of acute-type disease is made when the indolent-type and lymphoma-type are excluded, according to Shimoyama's criteria. The CD3 versus CD7 plot may discriminate the cases that will follow an indolent clinical course from the aggressive acute-type ATL.

The VL in each subpopulation indicated that HTLV-I-infected cells were relatively concentrated in the D and L subpopulations (representative data are shown in Figure 2A). These data are consistent with downregulation of CD3 and CD7 being relevant to HTLV-I infection, although cells without HTLV-I infection may also contribute to this change to some extent, as a substantial subpopulation of T cells has been reported to be CD7-deficient under physiological [23,24] and certain pathological conditions,

including autoimmune disorders and viral infection [25–29]. To more precisely analyze phenotypic changes in HTLV-I-infected cells, markers that indicate HTLV-I infection should be incorporated in future studies.

A summary of this study is shown in Figure 5. In the CD3 versus CD7 profile, most AC cases were included in Group 1, in which the D and L subpopulations were relatively small. Consistent with disease progression to smoldering- and chronic-type ATL, a decrease in the H subpopulation and increases in the D and L subpopulations occur (Group 2). In this step, increases in the sizes of clones in the D and L subpopulations are observed. Further expansion of the leukemic clone results in progression to acute-type ATL in which the L subpopulation has expanded (Group 3). According to a study by Yamaguchi *et al.*, the natural course of ATL is to progress from the HTLV-I carrier state through the intermediate state, smoldering ATL, and chronic ATL, and finally to the acute ATL, indicating a process of multistage leukemogenesis [19]. We consider this study to successfully link the progressive clinical status and phenotypic changes in HTLV-I-infected cells. However, the way in which this profile reflects multistep oncogenesis in HTVL-I infection at the molecular level remains unclear. Further molecular analyses of the three subpopulations will help in understanding the mechanism(s).

Supporting Information

Figure S1 Representative flow cytometric analysis of an HTLV-I asymptomatic carrier (patient no. 32). The CD3 versus CD7 plot of $CD4^+$ cells was constructed according to the gating procedure shown in this figure. In the plot, we designated three subpopulations: H ($CD3^{high}CD7^{high}$), D ($CD3^{dim}CD7^{dim}$), and L ($CD3^{dim}CD7^{low}$).
(PPTX)

Figure S2 A two-dimensional plot of 10 normal controls showing the percentage of the D and L subpopulations.
(PPTX)

Figure S3 Southern blot analysis of clonal integration of the HTLV-I provirus. Representative data (AC, No. 34) are shown. In *Eco*RI or *Pst*I digestion, a band indicated by a red arrow represents the monoclonal integration of the provirus. The band pattern indicates that two major clones coexist. This analysis was performed by a commercial laboratory (SRL, Tokyo, Japan).
(PPTX)

Table S1 Clinical data in a case of chronic-type ATL (No. 53). Proportion of abonormal lymphocytes in the preipheral blood WBC were evaluated by morphological exmanination. LDH: Lactate dehydrogenase (normal range, 120–240 U/L) sIL-2R: soluble interleukin-2 receptor (normal range, 122–496 U/ml).
(XLSX)

Acknowledgments

We thank Dr. Toshiki Watanabe, Dr. Kazumi Nakano, and Dr. Tadanori Yamochi (The University of Tokyo) for providing the TL-Om1 cell line and the plasmid containing the HTLV-I genome, which was used as a standard for the quantification of proviral load. We also thank Mr. Yuji Zaike (Clinical Laboratory, Research Hospital, Institute of Medical Science, The University of Tokyo) for his excellent technical advice. We are grateful to the hospital staff who have made a commitment to providing high-quality care to all of our patients.

Author Contributions

Conceived and designed the experiments: KT AT KU. Performed the experiments: SK YT. Analyzed the data: EW NW TI NO. Contributed reagents/materials/analysis tools: MI MT KU NO. Wrote the paper: SK KU.

References

1. Yoshida M, Miyoshi I, Hinuma Y (1982) Isolation and characterization of retrovirus from cell lines of human adult T-cell leukemia and its implication in the disease. Proc Natl Acad Sci U S A 79: 2031–2035.
2. Osame M, Usuku K, Izumo S, Ijichi N, Amitani H, et al. (1986) HTLV-I associated myelopathy, a new clinical entity. Lancet 1: 1031–1032.
3. Mochizuki M, Watanabe T, Yamaguchi K, Takatsuki K, Yoshimura K, et al. (1992) HTLV-I uveitis: a distinct clinical entity caused by HTLV-I. Japanese journal of cancer research : Gann 83: 236–239.
4. Proietti FA, Carneiro-Proietti AB, Catalan-Soares BC, Murphy EL (2005) Global epidemiology of HTLV-I infection and associated diseases. Oncogene 24: 6058–6068.
5. Yamaguchi K, Watanabe T (2002) Human T lymphotropic virus type-I and adult T-cell leukemia in Japan. International journal of hematology 76 Suppl 2: 240–245.
6. Murphy EL, Hanchard B, Figueroa JP, Gibbs WN, Lofters WS, et al. (1989) Modelling the risk of adult T-cell leukemia/lymphoma in persons infected with human T-lymphotropic virus type I. International journal of cancer Journal international du cancer 43: 250–253.
7. Shimoyama M (1991) Diagnostic criteria and classification of clinical subtypes of adult T-cell leukaemia-lymphoma. A report from the Lymphoma Study Group (1984–87). Br J Haematol 79: 428–437.
8. Tsukasaki K, Hermine O, Bazarbachi A, Ratner L, Ramos JC, et al. (2009) Definition, prognostic factors, treatment, and response criteria of adult T-cell leukemia-lymphoma: a proposal from an international consensus meeting. J Clin Oncol 27: 453–459.
9. Takasaki Y, Iwanaga M, Imaizumi Y, Tawara M, Joh T, et al. (2010) Long-term study of indolent adult T-cell leukemia-lymphoma. Blood 115: 4337–4343.
10. Hisada M, Okayama A, Shioiri S, Spiegelman DL, Stuver SO, et al. (1998) Risk factors for adult T-cell leukemia among carriers of human T-lymphotropic virus type I. Blood 92: 3557–3561.
11. Imaizumi Y, Iwanaga M, Tsukasaki K, Hata T, Tomonaga M, et al. (2005) Natural course of HTLV-1 carriers with monoclonal proliferation of T lymphocytes ("pre-ATL") in a 20-year follow-up study. Blood 105: 903–904.
12. Kamihira S, Atogami S, Sohda H, Momita S, Yamada Y, et al. (1994) Significance of soluble interleukin-2 receptor levels for evaluation of the progression of adult T-cell leukemia. Cancer 73: 2753–2758.
13. Iwanaga M, Watanabe T, Utsunomiya A, Okayama A, Uchimaru K, et al. (2010) Human T-cell leukemia virus type I (HTLV-1) proviral load and disease progression in asymptomatic HTLV-1 carriers: a nationwide prospective study in Japan. Blood 116: 1211–1219.
14. Okamoto T, Ohno Y, Tsugane S, Watanabe S, Shimoyama M, et al. (1989) Multi-step carcinogenesis model for adult T-cell leukemia. Japanese journal of cancer research : Gann 80: 191–195.
15. Matsuoka M, Jeang KT (2007) Human T-cell leukaemia virus type 1 (HTLV-1) infectivity and cellular transformation. Nat Rev Cancer 7: 270–280.
16. Yoshida M (2010) Molecular approach to human leukemia: isolation and characterization of the first human retrovirus HTLV-1 and its impact on tumorigenesis in adult T-cell leukemia. Proceedings of the Japan Academy Series B, Physical and biological sciences 86: 117–130.
17. Tian Y, Kobayashi S, Ohno N, Isobe M, Tsuda M, et al. (2011) Leukemic T cells are specifically enriched in a unique CD3(dim) CD7(low) subpopulation of CD4(+) T cells in acute-type adult T-cell leukemia. Cancer science 102: 569–577.
18. Sugamura K, Fujii M, Kannagi M, Sakitani M, Takeuchi M, et al. (1984) Cell surface phenotypes and expression of viral antigens of various human cell lines carrying human T-cell leukemia virus. International journal of cancer Journal international du cancer 34: 221–228.
19. Yamaguchi K, Kiyokawa T, Nakada K, Yul LS, Asou N, et al. (1988) Polyclonal integration of HTLV-I proviral DNA in lymphocytes from HTLV-I seropositive individuals: an intermediate state between the healthy carrier state and smouldering ATL. British journal of haematology 68: 169–174.
20. Mortreux F, Gabet AS, Wattel E (2003) Molecular and cellular aspects of HTLV-1 associated leukemogenesis in vivo. Leukemia : official journal of the Leukemia Society of America, Leukemia Research Fund, UK 17: 26–38.
21. Sasaki D, Doi Y, Hasegawa H, Yanagihara K, Tsukasaki K, et al. (2010) High human T cell leukemia virus type-1(HTLV-1) provirus load in patients with HTLV-1 carriers complicated with HTLV-1-unrelated disorders. Virology journal 7: 81.
22. Setoyama M, Katahira Y, Kanzaki T (1999) Clinicopathologic analysis of 124 cases of adult T-cell leukemia/lymphoma with cutaneous manifestations: the smouldering type with skin manifestations has a poorer prognosis than previously thought. The Journal of dermatology 26: 785–790.
23. Reinhold U, Abken H (1997) CD4+ CD7- T cells: a separate subpopulation of memory T cells? J Clin Immunol 17: 265–271.

24. Reinhold U, Abken H, Kukel S, Moll M, Muller R, et al. (1993) CD7- T cells represent a subset of normal human blood lymphocytes. J Immunol 150: 2081–2089.
25. Aandahl EM, Quigley MF, Moretto WJ, Moll M, Gonzalez VD, et al. (2004) Expansion of CD7(low) and CD7(negative) CD8 T-cell effector subsets in HIV-1 infection: correlation with antigenic load and reversion by antiretroviral treatment. Blood 104: 3672–3678.
26. Autran B, Legac E, Blanc C, Debre P (1995) A Th0/Th2-like function of CD4+CD7- T helper cells from normal donors and HIV-infected patients. J Immunol 154: 1408–1417.
27. Legac E, Autran B, Merle-Beral H, Katlama C, Debre P (1992) CD4+CD7-CD57+ T cells: a new T-lymphocyte subset expanded during human immunodeficiency virus infection. Blood 79: 1746–1753.
28. Schmidt D, Goronzy JJ, Weyand CM (1996) CD4+ CD7- CD28- T cells are expanded in rheumatoid arthritis and are characterized by autoreactivity. J Clin Invest 97: 2027–2037.
29. Willard-Gallo KE, Van de Keere F, Kettmann R (1990) A specific defect in CD3 gamma-chain gene transcription results in loss of T-cell receptor/CD3 expression late after human immunodeficiency virus infection of a CD4+ T-cell line. Proc Natl Acad Sci U S A 87: 6713–6717.

BJUI
BJU INTERNATIONAL

Risk of subsequent tumour recurrence and stage progression in bacille Calmette-Guérin relapsing non-muscle-invasive bladder cancer

Kazuhiro Matsumoto*†, Eiji Kikuchi*, Hiroshi Shirakawa*, Nozomi Hayakawa†‡, Nobuyuki Tanaka*, Akiharu Ninomiya†, Akira Miyajima*, So Nakamura† and Mototsugu Oya*

**Department of Urology, Keio University School of Medicine, †Department of Urology, Tokyo Saiseikai Central Hospital, and ‡Department of Urology, Tokyo Saiseikai Mukoujima Hospital, Sumida-ku, Tokyo, Japan*

Accepted for publication 8 February 2012

Study Type – Therapy (case series)
Level of Evidence 4

What's known on the subject? and What does the study add?
So far, few previous reports have analysed the risk factors for tumour recurrence and stage progression with a special focus on BCG-relapsing disease, defined as the recurrence after achieving a disease-free status by initial BCG instillations for 6 months. There are no guidelines outlining a specific treatment strategy for BCG-relapsing disease, although many BCG failure cases are attributable to BCG-relapsing disease.

In this study, additional BCG instillation was shown to decrease the subsequent tumour recurrence rate against BCG-relapsing tumours with intermediate pathological risk features; however, a BCG-relapsing tumour with a pathologically high risk was a significant risk factor for both subsequent tumour recurrence and stage progression. This information might identify a therapeutic strategy for BCG-relapsing tumours.

OBJECTIVE

- To investigate the risk of subsequent tumour recurrence and stage progression in bacillus Calmette-Guérin (BCG)-relapsing non-muscle-invasive bladder cancer, defined as recurrence after achieving a disease-free status for 6 months.

PATIENTS AND METHODS

- A total of 183 patients with BCG-relapsing tumours were treated with conservative therapy between 1985 and 2008 at our three institutions.
- We analysed the association between their clinicopathological parameters and subsequent tumour recurrence or stage progression.

RESULTS

- Additional induction courses of BCG or anticancer drug (mitomycin C or epirubicin) instillations were performed in 119 patients and 24 patients, respectively. The remaining 40 patients did not undergo any adjuvant therapy.
- Multivariate analysis showed that a relapsing tumour with a pathologically high risk (defined as tumours with G3 and/or pT1 and/or concomitant carcinoma *in situ*) was a significant risk factor for subsequent tumour recurrence ($P = 0.002$; hazard ratio [HR] 2.15). Additional BCG instillation significantly decreased the subsequent tumour recurrence rate ($P < 0.001$; HR 0.41).
- Multivariate analysis also showed that a relapsing tumour with a pathologically high risk was also significantly associated with stage progression ($P < 0.001$; HR 8.05).

CONCLUSIONS

- An additional course of BCG instillation might be effective in patients with BCG-relapsing tumours with pathologically intermediate risk.
- Nevertheless, some patients with high-risk pathological features developed subsequent stage progression. Such patients should be followed up closely and counselled on the need for aggressive therapeutic options, such as radical cystectomy.

KEYWORDS

BCG relapsing, tumour recurrence, stage progression, bacille Calmette-Guérin, BCG failure, non-muscle-invasive bladder cancer

INTRODUCTION

Initially diagnosed intermediate- or high-risk non-muscle-invasive bladder cancer (NMIBC) with stage Ta or T1 papillary carcinoma and/or carcinoma *in situ* (CIS) are usually treated by transurethral resection of bladder tumour (TURBT) and adjuvant BCG immunotherapy to prevent tumour recurrence. Based on the results of several randomized trials, it has become obvious that intravesical BCG instillation, with or without maintenance therapy, is the effective therapy of choice for intermediate- or high-risk NMIBC, and BCG is now known to be superior to other

intravesical agents for the prevention of tumour recurrence [1–4]. However, some patients treated with BCG therapy still suffer from recurrence and, in the most general sense, any disease appearance after BCG therapy can be referred to as 'BCG failure'. Current therapeutic options for BCG failure cases are radical cystectomy or additional intravesical therapy (repeat BCG treatment or other intravesical chemotherapy) [5]. In previous reviews of patients who underwent radical cystectomy for high-risk NMIBC after BCG failure, 5-year disease-specific survival rates ranged from 60 to 79% [6–8]. Nevertheless, despite the potentially curative nature of cystectomy, many physicians and patients may prefer to delay cystectomy in favour of preserving bladder function. O'Donnell and Boehle [9] reviewed previous published studies and calculated that ≈35% (76/157) of patients failing the first course of BCG achieve durable success with another BCG cycle. In other studies that examined additional chemo-instillation for BCG failure cases with shorter follow-up periods, the recurrence-free rates at 24 months ranged from ≈20 to 30% with gemcitabine [10] or mitomycin C (MMC) [11]. Steinberg *et al.* [12] performed intravesical instillation of valrubicin in 90 CIS patients with BCG failure and reported a complete response rate at 6 months of 21%.

In the above-mentioned studies, BCG failure was inconsistently defined and included very heterogeneous populations with various natural histories. Herr and Dalbagni [13] noted that comparisons between therapies have been hampered by the lack of a standard definition for BCG failure. To provide more uniformity in reporting, Nieder *et al.* [14] advocated that the following alternative descriptive terms for specific types of BCG failure should be used whenever possible. They divided BCG failure into four different defined types. BCG-refractory disease is the term used when there is failure to achieve a disease-free state by 6 months after initial BCG therapy because of either persistent or rapidly recurrent disease. BCG-resistant disease is recurrence or persistence of disease at 3 months after the induction cycle. It is of lesser degree, stage or grade, and is no longer present at 6 months from BCG retreatment. BCG-relapsing disease is defined as recurrence of disease after achieving a disease-free state by 6 months. BCG-intolerant disease is the term used when disease recurs after a less-than-adequate course of therapy is applied because of a serious adverse event or symptomatic intolerance.

There is growing consensus that early cystectomy is beneficial for BCG-refractory disease [13]. By contrast, it is unclear how we should treat BCG-relapsing disease, although many BCG failure cases are attributable to BCG-relapsing disease. In the present study, we reviewed and focused on 183 patients with BCG-relapsing tumours, who were treated with conservative therapy, to analyse their subsequent tumour recurrence and stage progression. These data should assist with the establishment of an appropriate therapeutic strategy for patients with BCG-relapsing disease.

PATIENTS AND METHODS

PATIENT SELECTION

We identified a total of 280 patients with BCG failure with NMIBC between 1985 and 2008 at our three institutions, 253 of whom were treated with conservative therapy (45 patients with BCG-refractory, three patients with BCG-resistant, 22 patients with BCG-intolerant, and 183 patients with BCG-relapsing disease). A retrospective study was then conducted in the 183 patients with BCG-relapsing disease (149 men and 34 women) with diagnosed NMIBC (pTa or pT1) recurrence after a previous complete response to a single induction course of BCG therapy (6–8 instillations). The median (range) follow-up interval after BCG relapsing was 5.1 (0.4–15.2) years and the mean (range) age of the patients at BCG relapsing was 67.3 (31.8–89.7) years.

TREATMENT AND FOLLOW-UP

These cases were routinely assessed by urine cytology and cystoscopy every 3 months for the first 2 years after TURBT, every 6 months for the next 3 years, and every 6–12 months thereafter. I.v. urography, ultrasonography, and/or CT were used to evaluate the bladder and upper urinary tract every year for the first 5 years and then every 1 or 2 years thereafter. BCG treatment at a dose of 81 mg (Connaught strain), 80 or 40 mg (Tokyo 172 strain), MMC at a dose of 30 mg, or epirubicin at a dose of 50 mg was begun 4 to 5 weeks after TURBT and continued weekly for 6–8 weeks. The starting point of this study was the timing of TURBT for a relapsing tumour and the endpoint was subsequent tumour recurrence or stage progression. Recurrence was defined as a new tumour appearing in the bladder after clearance. Progression was defined as confirmed histological muscle invasion (pathological stage T2 or higher disease) or detectable distant metastases.

CLINICOPATHOLOGICAL RISK STRATIFICATION

The characteristics of tumour grade, number of tumours, pathological stage and the presence of CIS were determined. Referring to the current published AUA guidelines [15] we divided the patients into three clinicopathological risk groups. We constructed this risk stratification by interpreting low grade as G1-2 and high grade as G3. Tumour size was excluded from the analysis because some of the data contained inaccurate measurements. The pathological high risk cases were defined as tumours with G3 and/or pT1 and/or concomitant CIS. Multiple and/or recurrent G1-2 pTa tumours were considered to be intermediate-risk tumours. Initial and solitary tumours with G1-2 pTa were considered to be low-risk tumours; therefore, the BCG-relapsing tumours were inevitably classified as high- or intermediate-risk tumours because they were all recurrent tumours.

STATISTICAL ANALYSIS

The chi-squared test was used to analyse the difference between two groups. Recurrence-free and progression-free survival curves were constructed using the Kaplan–Meier method, and were compared with the log-lank test. Differences among groups were regarded as significant when $P < 0.05$. To determine risk factors for subsequent recurrence or progression, univariate and multivariate analyses were performed using the Cox proportional hazards model with stepwise forward selection.

RESULTS

PATIENT CHARACTERISTICS AND TREATMENT

For patients with BCG relapsing, additional induction courses of BCG instillations were

performed in 119 patients, and 24 patients received intravesical chemotherapy (18 MMC and six epirubicin). The remaining 40 patients did not undergo any adjuvant therapy. BCG relapsing was further defined by time of recurrence as early (within 12 months), intermediate (12 to 24 months) or late (>24 months) [14]. The clinical characteristics of the patients with BCG-relapsing tumours are listed in Table 1. No adjuvant therapy tended to be chosen in patients with a clinicopathological intermediate-risk tumour in the relapsing tumour group, compared with the BCG and chemotherapy groups. In the additional BCG therapy group for BCG-relapsing tumours (119 patients), 60 patients (50.4%) had clinicopathologically high risk tumours in the previous tumours and 66 patients (55.5%) had clinicopathologically high risk tumours in the BCG-relapsing tumours. Among the 24 patients treated with additional chemotherapy instillation for a BCG-relapsing tumour, 18 (75.0%) had clinicopathologically high risk tumours in the previous tumours and 13 (54.2%) had clinicopathologically high risk tumours in the BCG-relapsing tumours.

TABLE 1 Clinicopathological backgrounds of patients with BCG-relapsing disease

	Intravesical therapy for BCG-relapsing tumours		
	BCG	Chemotherapy	None
Total no. of patients	119	24	40
Mean age at BCG relapsing, years	**66.6**	**67.8**	**69.7**
Gender, *n* (%)			
Male	100 (84.0)	17 (70.8)	32 (80.0)
Female	19 (16.0)	7 (19.2)	8 (20.0)
Clinicopathological risk group of the previous tumour, *n* (%)*‡			
High	60 (50.4)	18 (75.0)	17 (32.5)
Intermediate	51 (42.9)	4 (16.7)	20 (50.0)
Low	8 (6.7)	2 (8.3)	3 (7.5)
Pathological stage, *n* (%)*‡			
pTa	84 (70.6)	11 (45.8)	29 (72.5)
pT1	35 (29.4)	13 (54.2)	11 (27.5)
Grade, *n* (%)			
Grade 1/2	79 (66.4)	14 (58.3)	24 (60.0)
Grade 3	40 (33.6)	10 (41.7)	16 (40.0)
Multiplicity, *n* (%)*‡			
Solitary	27 (22.7)	12 (50.0)	9 (22.5)
Multiple	92 (77.3)	12 (50.0)	31 (77.5)
Concomitant CIS†			
Yes	29 (24.4)	3 (12.5)	3 (7.5)
No	90 (75.6)	21 (87.5)	37 (92.5)
Timing of relapsing, *n* (%)*‡			
Early	35 (29.4)	13 (54.2)	8 (20.0)
Intermediate	36 (30.3)	5 (20.8)	14 (35.0)
Late	48 (40.3)	6 (25.0)	18 (45.0)
Clinicopathological risk group of the relapsing tumour, *n* (%)†‡			
High	66 (55.5)	13 (54.2)	10 (25.0)
Intermediate	53 (44.5)	11 (45.8)	30 (75.0)
Pathological stage, *n* (%)†‡			
pTa	84 (70.6)	16 (66.7)	35 (87.5)
pT1	35 (29.4)	8 (33.3)	5 (12.5)
Grade, *n* (%)†‡			
Grade 1/2	74 (62.2)	14 (58.3)	33 (82.5)
Grade 3	45 (37.8)	10 (41.7)	7 (17.5)
Multiplicity, *n* (%)			
Solitary	52 (43.7)	11 (45.8)	21 (52.5)
Multiple	67 (56.3)	13 (54.2)	19 (47.5)
Concomitant CIS, *n* (%)†			
Yes	21 (17.6)	4 (16.7)	2 (5.0)
No	98 (82.4)	20 (83.3)	38 (95.0)

*Statistical difference of populations; *BCG group vs chemotherapy group* $P < 0.05$*; †BCG group vs no adjuvant group* $P < 0.05$*; ‡Chemotherapy group vs no adjuvant group* $P < 0.05$.

SUBSEQUENT TUMOUR RECURRENCE

Overall, 82 patients with BCG-relapsing disease (44.8%) experienced subsequent tumour recurrence during the follow-up periods. To identify significant risk factors for subsequent tumour recurrence, we performed univariate and multivariate analyses using the Cox proportional hazard model with stepwise forward selection. As shown in Table 2, additional BCG instillation was shown to significantly decrease the rate of subsequent tumour recurrence ($P < 0.001$; hazard ratio [HR], 0.41; 95% CI, 0.23–0.72), and a clinicopathologically high risk of the relapsing tumour ($P = 0.002$; HR, 2.15; 95% CI, 1.33–3.49) was selected as a significant unfavourable risk factor for subsequent tumour recurrence. As seen in Fig. 1a, the 5-year recurrence-free survival rates were 59.8% in the BCG group, 21.6% in the chemotherapy group, and 43.1% in the no adjuvant therapy group. In the 119 patients who underwent an additional induction course of BCG therapy, the 5-year recurrence-free survival rate was 77.6% in the intermediate-risk group and 46.3% in the high-risk group ($P = 0.025$ [Fig. 1b]).

SUBSEQUENT STAGE PROGRESSION

In the follow-up periods, subsequent stage progression was observed in 25 patients (13.7%). In 19 (76.0%) of these 25 patients, stage progression was found with muscle-invasive bladder tumours without any metastases. Radical cystectomy was performed in 12 patients, three of whom later died from bladder cancer. Three other patients were treated with local radiation therapy; two patients were still alive, and one died from bladder cancer. One elderly patient also died from bladder cancer after being treated with supportive care alone. The treatments and prognoses of the

TABLE 2 Univariate and multivariate analyses for tumour recurrence and stage progression in the BCG-relapsing tumour group

	Recurrence			Progression		
	Univariate	Multivariate		Univariate	Multivariate	
	P	*P*	HR (95%CI)	*P*	*P*	HR (95%CI)
Age	0.277			0.865		
Gender	0.939			0.638		
Male ($n = 149$) vs female ($n = 34$)						
Clinicopathological risk group of the prior tumour	**0.009**			**0.002**		
High ($n = 95$) vs intermediate /low ($n = 88$)						
Timing of relapsing	**0.043**			0.803		
Early ($n = 56$) vs intermediate/late ($n = 127$)						
Clinicopathological risk group of the relapsing tumour	**0.026**	**0.002**		**<0.001**	**<0.001**	
High ($n = 89$) vs			**2.15 (1.33–3.49)**			**8.05 (2.74–23.6)**
intermediate ($n = 94$)			**1.00**			**1.00**
Intravesical therapy	**0.001**	**<0.001**		0.886		
BCG ($n = 119$) vs			**0.41 (0.23–0.72)**			
chemotherapy ($n = 24$) vs			**1.28 (0.65–2.52)**			
not done ($n = 40$)			**1.00**			

remaining three patients who had local invasive disease without distant metastases and were treated at other hospitals are unknown. Meanwhile, six of 25 stage progression cases (24.0%) were diagnosed with metastatic disease. Five were treated with systemic chemotherapy and one elderly patient was treated with supportive care alone; however, all six eventually died from bladder cancer. Univariate and multivariate analyses were performed again to evaluate the risk factors for stage progression (Table 2). The results indicated that a clinicopathologically high risk relapsing tumour ($P < 0.001$; HR, 8.05; 95% CI, 2.74–23.6) was significantly associated with subsequent stage progression. The 5-year progression-free survival rate was 97.7% in the intermediate-risk group and 72.2% in the high-risk group ($P < 0.001$ [Fig. 1c]). Kaplan–Meier curves of the cancer-specific survival rates showed the 5-year cancer-specific survival rates were 98.9% and 87.9% in the intermediate- and high-risk groups, respectively ($P = 0.006$ [Fig. 1d]). However, we could not find significant differences in the progression-free survival rates (Fig. 1e) and cancer-specific survival rates (Fig. 1f) among the BCG group, chemotherapy group and no adjuvant group.

DISCUSSION

In the present study, special attention was focused on BCG relapsing, which is defined as the recurrence of disease after achieving a disease-free status by 6 months. Until now, few previous reports have analysed risk factors for subsequent tumour recurrence and stage progression with a special focus on BCG-relapsing disease. In the present study, we evaluated 183 patients with BCG-relapsing disease treated by conservative therapy with a long follow-up. An important finding was that a BCG-relapsing tumour with a pathologically high risk was a significant unfavourable factor for both subsequent tumour recurrence and stage progression, and it could be used to clearly differentiate the prognosis. Additional BCG instillation proved to decrease the subsequent tumour recurrence rate compared with the chemotherapy group and the no adjuvant group.

A few previous reports have described treatment options for BCG-relapsing disease. Repeat BCG treatment for BCG-relapsing tumours was reported by Brake *et al.* [16] who found that 19 of 24 patients who had BCG-relapsing tumours remained tumour free, while four patients experienced stage progression with a median interval of 2 years, although their definition of a BCG-relapsing tumour was recurrence after achieving disease-free status 3 months after the first BCG therapy. Bui *et al.* [17] also described 11 patients with BCG-relapsing tumours (recurrence 9–74 months after the first BCG therapy) who received a second induction course of BCG, all of whom experienced tumour recurrence after a 6-month disease-free status. Five of their 11 patients continued to be disease-free until the last follow-up at a median of 87 months.

There are no guidelines outlining a specific treatment strategy for BCG-relapsing disease. The AUA guidelines recommend radical cystectomy for BCG failure cases, but they also state that repeat BCG intravesical therapy may be appropriate in patients who develop a late recurrence after a previous complete response to an intravesical agent [15]. The National Comprehensive Cancer Network guidelines recommend radical cystectomy, changing the intravesical agent to MMC, valrubicin, gemcitabine or BCG plus interferon, or maintenance BCG to treat tumour recurrence after BCG therapy [18]. The European Association of Urology guidelines strongly recommend immediate cystectomy for BCG failure because of the high risk for stage progression. They also state that changing from BCG to intravesical chemotherapy or device-assisted chemotherapy instillations can yield responses in selected cases [19]. Boström *et al.* [20] commented, in their review, that if there is a significant tumour-free period, re-induction of BCG may be considered. However, clinical data to support these recommendations are insufficient and further investigation and validation of results seem to be warranted to establish

the efficacy of these second-line therapies, especially for BCG-relapsing cases.

An additional course of BCG instillation might be effective in patients with BCG-relapsing tumours that have intermediate-risk pathological features as this may help prevent subsequent tumour recurrence to a significant degree compared with the chemotherapy group and the no adjuvant group. We concluded that they could be relatively safely treated by conservative therapy with additional BCG instillations, and few patients experienced subsequent stage progression. However, some patients with BCG-relapsing tumours with high-risk pathological features treated with conservative therapy developed subsequent stage progression, and the 5-year cancer-specific death rate was 12.1%. Such patients should be followed up closely and counselled on the possible need for aggressive therapeutic options, such as radical cystectomy.

The present study has several limitations. First, it was performed in a retrospective fashion and in a limited number of patients. The preference of the attending doctor dictated what kind of intravesical adjuvant therapy was to be performed. Disparities in the backgrounds of the patients among the groups of intravesical therapies could prevent a fair comparison between these groups and may have introduced bias into the results. Another limitation is that a second TUR was not performed in this period. Furthermore, maintenance BCG therapy was not performed in patients in the present study, which is increasingly accepted owing to its positive impact on both recurrence and progression [21], and this may limit the generalizability of the results. The results of the meta-analysis performed by Sylvester *et al.* [3] showed that the effect of BCG on progression was limited to the trials in which some form of BCG maintenance was used, and no reduction was seen in the trials where maintenance BCG was not used. Therefore, if maintenance BCG therapy is performed for a BCG-relapsing tumour, we might be able to reduce the subsequent tumour recurrence rate and even the stage progression rate more than the present results. In a future study, it would be of great interest to evaluate the effect of maintenance BCG therapy in patients with a BCG-relapsing tumour for reducing

*Fig. 1. (**a**) Differences in subsequent tumour recurrence-free survival rates among the patients with BCG-relapsing disease treated with intravesical BCG therapy, intravesical chemotherapy, and no adjuvant therapy. The time point zero was the timing of TURBT for relapsing tumours. (**b**) Differences in subsequent tumour recurrence-free survival rates according to the pathological risk features of BCG-relapsing tumours in 119 patients who received an additional induction course of BCG. (**c**) Differences in subsequent progression-free survival rates according to the pathological risk features of BCG-relapsing tumours in all 183 study patients. (**d**) Differences in cancer-specific survival rates according to the pathological risk features of BCG-relapsing tumours in all 183 study patients. (**e**) Differences in subsequent progression-free survival rates among the patients with BCG-relapsing disease treated with intravesical BCG therapy, intravesical chemotherapy, and no adjuvant therapy. (**f**) Differences in cancer-specific survival rates among the patients with BCG-relapsing disease treated with intravesical BCG therapy, intravesical chemotherapy, and no adjuvant therapy.*